MAPPING CRUSTAL TERRANE BOUNDARIES IN MANICOUAGAN QUEBEC

MAPPING CRUSTAL TERRANE BOUNDARIES IN MANICOUAGAN QUEBEC, OF THE GRENVILLE PROVINCE: CHARACTERIZATION OF ISOTOPIC SIGNATURES FROM DIFFERING CRUSTAL SOURCES AND EVIDENCE FROM AEROMAGNETIC DATA

By

STEPHANIE D. THOMSON, B.Sc (Hons.)

A Thesis

Submitted to the School of Graduate Studies

In Partial Fulfillment of the Requirements

For the Degree

Master of Science

McMaster University

MASTER OF SCIENCE (2009)	McMaster University
(Earth Science)	Hamilton, Ontario

TITLE:	Mapping crustal terrane boundaries in Manicouagan Quebec, of the Grenville Province: Characterization of isotopic signatures from differing crustal sources and evidence from aeromagnetic data
AUTHOR:	Stephanie D. Thomson, B.Sc (McMaster University)
SUPERVISOR:	Professor Alan P. Dickin
NUMBER OF PAGES:	87, xi

ABSTRACT

The Grenville Province is a 1Ga orogenic belt, composed of much older terranes whose age and extent require mapping in order to gain a better understanding of its geological evolution. Manicouagan, Quebec, in the Grenville Province, has experienced several orogenic events, as well as being the site of a 214 Ma hypervelocity impact event, which has further complicated its geological structure. By analyzing surface samples from this area, as well as drill core of the country rocks involved in the impact, the original age of crustal formation for the various terranes can be calculated, thus revealing the evolutionary history of the Manicouagan area.

Nd isotopes are resistant to metamorphic disturbances, therefore permitting accurate calculations of original crustal formation ages. Nd-isotopic analysis of granitoid orthogneisses, has identified three major crustal formation age groups in the area. These are: Mesoproterozoic (1.58 Ga), Paleoproterozoic (1.86 Ga), and Archean (2.8 Ga). These average depleted mantle model ages (T_{DM}) correspond well with isochron reference lines, supporting their validity as actual geologic events.

The spatial distribution of age data results indicate that the Archean basement extends farther south on the western side of the Manicouagan reservoir than previously thought, whereas the eastern side is dominated by Paleoproterozoic crust. In contrast, the Manicouagan Imbricate Zone (MIZ), located between the Archean and Paleoproterozoic crustal terranes, has a wider scatter of Nd data attributed to mixing between Archean and Proterozoic sources. This crustal terrane has been limited to within the interior of the reservoir in the south, and extends just north of the reservoir. The location of the

boundary between the Archean and Paleoproterozoic terranes, the Allochthon Boundary Thrust (ABT), was largely agreed upon to the east and west of the impact, but its position was highly ambiguous near the impact itself. New Nd analysis shows that this boundary crosses onto the island on the NW side of the reservoir, and exits to the west of the previously established Cryptic Shear Zone (CSZ) at the southern end of the impact. The boundaries of these distinctive crustal terranes are further supported through aeromagnetic evidence.

The 214 Ma hypervelocity event resulted in the instantaneous melting of target rocks located beneath the impact. Isotopic and elemental geochemistry was employed to characterize the composition of the meltsheet. These data show that the melt sheet was largely derived from the MIZ, but cannot rule out a small component of underlying Archean crust. Further isotopic, trace element and major elemental analyses are needed in order to fully decipher the target rock composition.

ACKNOWLEDGEMENTS

I would like to thank my supervisor Dr. Alan Dickin for his continual support and encouragement for the duration of this project. I would also like to thank Dr. Spray for allowing access to the Manicouagan drill core, and Dr. Morris and Hernan Ugalde for their assistance with the aeromagnetic data. To my fellow lab mates: Esther Moore, Rebecca Hewitson, Eden Hynes and Mark Zelek, your help has seen invaluable!! (and not only because without these very special people, many samples would be still waiting for HF!) Finally, I would like to thank my family an friends who have continued to support me through the years and studies.

TABLE OF CONTENTS

LIST OF FIGURES

LIST OF TABLES

CHAPTER 1: GEOLOGIC BACKGROUND

1.0 Introduction

The Grenville Province is the youngest geologic province of the Canadian Shield. It is a product of several orogenic cycles, and therefore can be described as a composite of several crustal terranes with distinctive histories. These cycles include pre-Grenvillian arc-continent collisions on the margin of Laurentia, such as the Labradorian orogeny (1680-1450 Ma), Pinwarian Orogeny (1500-1450 Ma), and the Elzevirian Orogeny (1250-1190 Ma), in addition to the continent-continent collision of the Grenvillian Orogeny (1160-970 Ma) (Rivers, 1997). Each of these events was accompanied by magmatic and metamorphic reworking of older crustal units. As a result, much of the geological evidence used to distinguish the evolutionary history of the region has been masked or even erased. Through the use of Nd isotope analysis, it is possible to calculate the original age of formation for distinct crustal terranes, thereby uncovering important aspects of the evolutionary history of the Grenville Province.

The Grenville Orogeny is characterized by several different pulses of crustal shortening and metamorphism, sometimes followed by crustal extension (Indares et. al., 2000). It was terminated by the collision with another continent, which, based on geochronological and plate reconstruction evidence, was likely South America (Rivers 1997). These pulses occurred at approximately 1190-1140 Ma (Shawinigan), 1080-1020Ma (Ottawan), and 1000-980 Ma (Rigolet) (Rivers, 1997), and resulted in the current configuration of the Grenville Province.

1.1.0 Structural Belts of the Grenville Province

According to the model of Rivers et al. (1989), the Grenville Province is made of three distinctive sub-parallel belts running the length of the province, each separated by a thrust zone. The three major belts are: the Parautochthonous belt, the Allochthonous Polycyclic Belt, and finally the Allochthonous Monocyclic Belt. These are bounded by thrust zones including the Grenville Front, the Allochthon Boundary Thrust (ABT) and the Monocyclic Belt Boundary Zone (MBBZ).

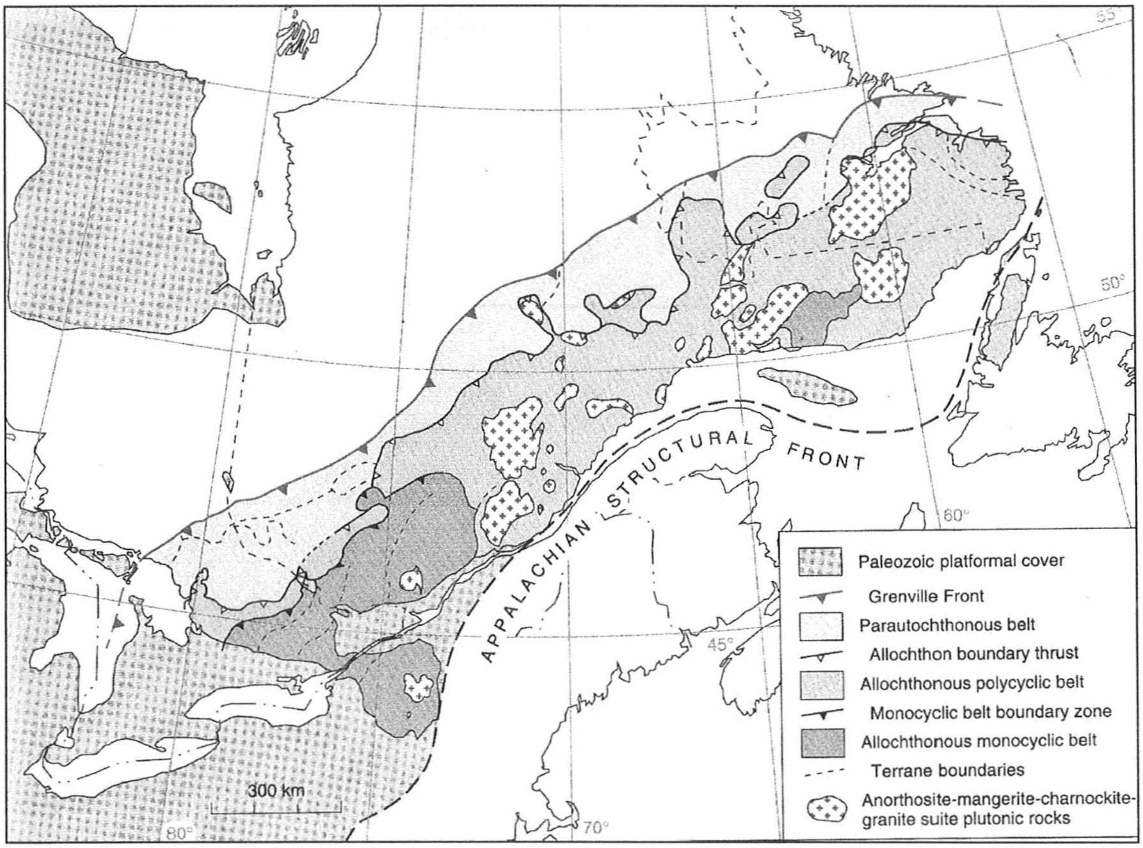

Figure 1.1: Structural Belts of the Grenville Province (after Davidson, 1998)

1.1.1 The Grenville Front

The Grenville Front marks the farthest northwesterly boundary of the Grenville Province, separating the Archean crust of the Superior Province from reworked Archean crust of the Grenville Parautochthon. It is a 2000 km long thrust zone, which often interrupts metamorphic signatures and faulting patterns between the two Provinces (Rivers et al. 1989).

1.1.2 Parautochthon

The Grenville Orogeny effectively overprinted the SE margin of already metamorphosed Archean crust, giving rise to a belt of reworked Archean crust which has nevertheless not been subjected to major horizontal transport (Indares et al. 2000). Although much of this belt has undergone intense metamorphism, some geologic structures still remain and can be correlated to those found in the autochthon on the other side of the Grenville Front. Overall, the metamorphic grade across this reworked Archean crustal belt increases to the southeast (Rivers et al. 1989).

1.1.3 Allochthon Boundary Thrust

The Allochthon Boundary Thrust (ABT) is termed a crustal scale ramp, which may extend through the whole thickness of the crust, as well as along the entire length of the Province, running sub-parallel to the Grenville Front (Rivers, 1997). This thrust zone separates reworked Archean - Paleoproterozoic crust from the Paleoproterozoic – Mesoproterozoic crust thrust over it. It has been documented by means of structural, metamorphic, geochronologic and magnetic mapping, although its location remains ambiguous in some areas of the Grenville (Rivers et al. 1989).

1.1.4 Polycyclic Allochthon

During the Paleoproterozoic and Mesoproterozoic, several orogenic cycles resulted in the accretion of multiple allochthonous terranes to the Laurentian margin. These terranes became increasingly metamorphosed during subsequent accretionary events, including the final Grenville terminal orogeny. The Allochthonous Polycyclic Belt refers to terranes along the length of the Grenville Province with a high metamorphic grade ranging from amphibolite to granulite facies as a result of having experienced multiple orogenic cycles (Rivers et al. 1989).

1.1.5 Monocyclic Belt Boundary Zone

The Monocyclic Belt Boundary Zone (MBBZ) is a tectonic zone separating the southeastern terranes of the Allochthonous Monocyclic Belt from the Polycyclic Allochthon. The northwestward thrusting of the monocyclic belt over the polycyclic belt has been dated to 1060 Ma, a time that coincides with deformation in the underlying polycyclic basement (Rivers et al. 1989).

1.1.6 Monocyclic Allochthon

The Allochthonous Monocyclic Belt is composed of Mesoproterozoic crust that has been involved in only one accretionary metamorphic event. This occurs in the southeastern part of the province, in Southern Ontario, and largely corresponds in extent to the Central Metasedimentary Belt (CMB) of Wynne Edwards (1972). The CMB has been the subject of multiple evolutionary models, including an interpretation as the Composite Arc Belt proposed by Carr et al. (2000). The CMB is characterized by a series of supracrustal assemblages including an abundance of Grenville marbles, in addition to volcanic rocks, platformal and continental margin deposits (Rivers et al. 1989). Hanmer et al. (2000) proposed that, due to older Nd model ages (consistently > 1.35Ga) found on both the northwest and the southeast sides of the CMB, the area is likely a result of the opening of a back arc basin. This model was modified by Dickin and McNutt (2007) to a back-arc rift zone. The extensive marbles and other supracrustal assemblages in the area support this back arc model, as this allows the opportunity for a marine environment to deposit such lithologic packages between the older gneiss units flanking this region.

1.2 Geologic Setting of the Manicouagan Study Area

The Manicouagan region is located in central Quebec (Figure 1.2). As part of the Grenville Province, Manicouagan has experienced several orogenic events, producing highly metamorphosed crust and obscuring many earlier geologic features. Of the three structural belts in the Grenville Province, only the parautochthon and the polycyclic allochthon are present in the Manicouagan study area. However, Grenville thrusting in this region has resulted in areas that have experienced very high pressure metamorphism that is poorly understood. In addition, the site has undergone a meteorite impact, which has even further complicated the geologic history of the crust within Manicouagan by masking the boundaries between the older crustal units.

The impact occurred at approximately 214 Ma and the resulting impact structure is approximately 100 km in diameter. It has a melt sheet up to 230 m thick that lies directly over the ABT. Beneath the melt sheet suevitic breccias of shock metamorphosed basement clasts, glass fragments, and fragmented target rocks continue to obscure the pre-impact geology (Dressler and Reimold, 2001).

The geological investigation of the crustal "target units" below and around the impact melt sheet is of value in modeling the origin of the melt sheet itself. Therefore, this question will be examined in a later chapter, after characterization of the main crustal units in the area.

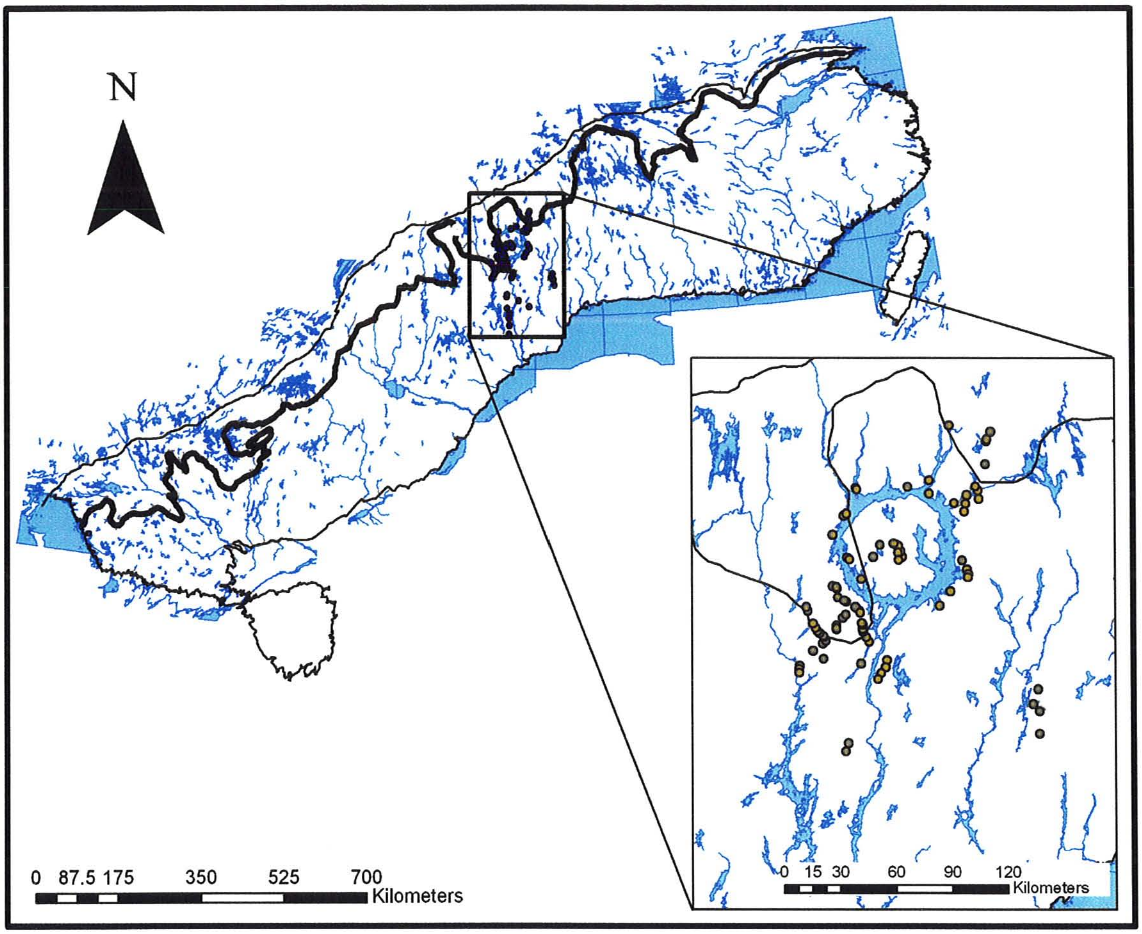

Figure 1.2: Location of the Manicouagan study area in the Grenville Province. Black line traversing the study area is the proposed location of the ABT. (NTDB, 2006)

1.2.1 Geologic Terranes

Based on geological and structural mapping summarized by Hynes et al. (2000), the Manicouagan area has been divided into several structural terranes (Figure 1.3). These include: the Gagnon Terrane on parautochthonous Archean basement, and four allochthonous terranes; Hart Jaune Terrane, Berthé Terrane, and the Manicouagan Imbricate Zone (made up of the Lelukuau and Tshenukutish Terranes). These terranes each differ in lithology and evolutionary history.

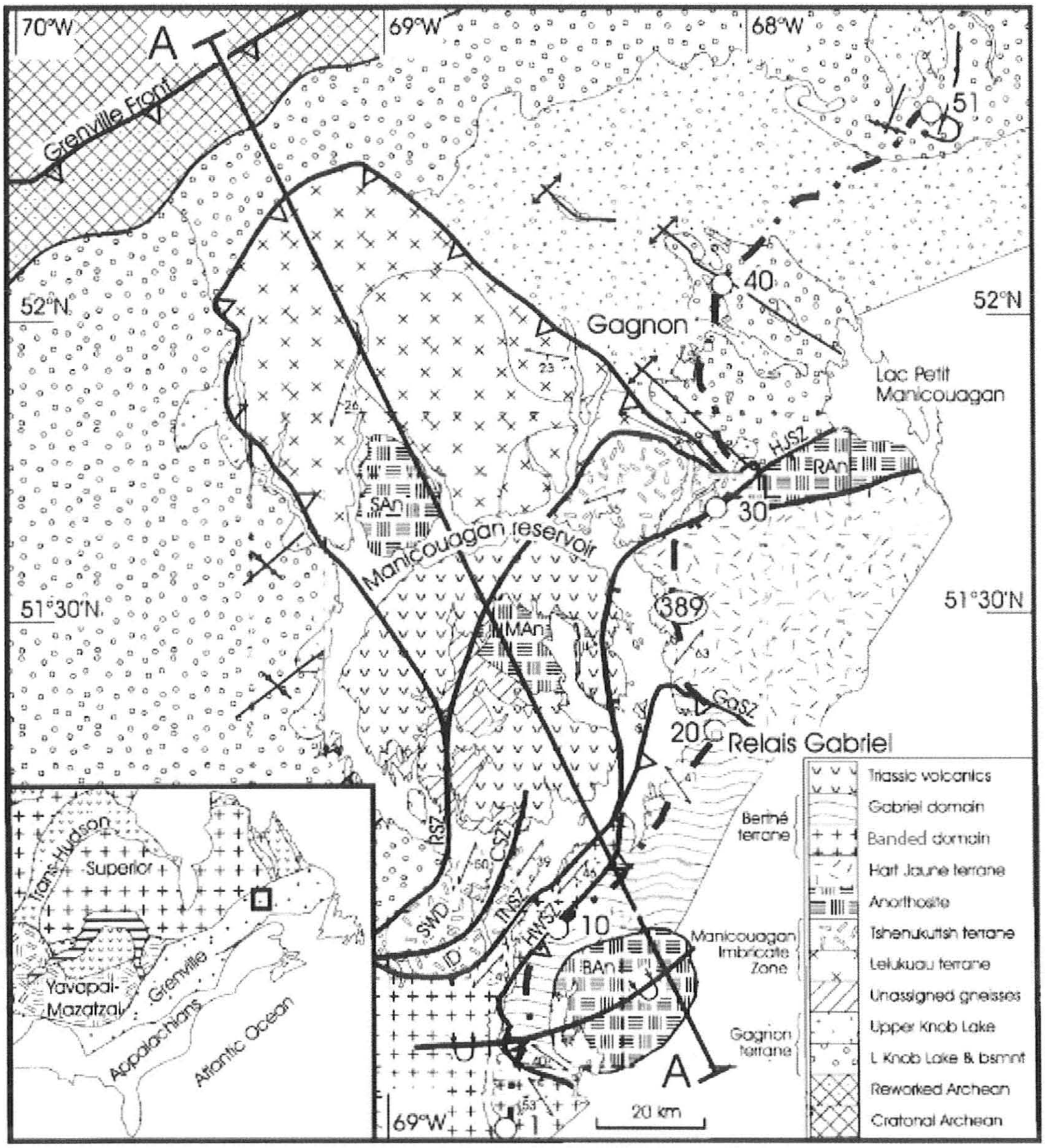

Figure 1.3: Terranes of the Manicouagan Area as proposed by Hynes et al. (2000). Shear zones include: Cryptics Shear Zone (CSZ), Relay Shear Zone (RSZ), Gabriel Shear Zone (GaSZ), Hart Jaune Shear Zone (HJSZ), Triple Notch Shear Zone (TNSZ). Boundaries have been modified since (Indares et al. 2002, 2004), however overall model remains the same.

1.2.1 Gagnon Terrane

As previously mentioned, the Gagnon Terrane is the only terrane located on an Archean basement. It is composed of Paleoproterozoic metasediments of the Knob Lake Group. These include: quartzofeldspathic schist and gneiss derived from greywacke deposited in a deeper marine environment, as well as marble, quartzite and a banded iron formation, which were deposited in shallower marine environments (Rivers and Chown, 1986). The reworked Archean basement is largely composed of strongly foliated, granoblastic quartzfeldspathic gneiss with mafic layers.

On the western side of the Gagnon Terrane, the supracrustal rock assemblages and the underlying Archean basement form imbricated thrust sheets. These thrust sheets are believed to have occurred during the Grenvillian orogeny, when deep seated faulting exhumed Archean crust through the overlying metasediments (Hynes and Eaton, 1999). The reworked Archean gneiss and the overlying metasedimens of the Gagnon Terrane are often indistinguishable from each other in the field. Monzonite U-Pb ages have been calculated for the terrane, which yield metamorphic ages of 1720-1740 Ma. The Gagnon Terrane is truncated to the south by the Relay Shear Zone (RSZ), which separates the Archean basement from the structurally overlying Manicouagan Imbricate Zone, and represents the local manifestation of the ABT.

1.2.1.2 Manicouagan Imbricate Zone

The Manicouagan Imbricate Zone (MIZ) is thought to underlie most of the impact crater, surfacing in a large lobe to the north of the impact. It is thrust over the Gagnon Terrane in the north and is overthrust by the Hart Jaune Terrane and Berthé Terrane in the east and southeast.

Through the use of seismic reflection profiling, the MIZ has been modeled as a shallow dipping crustal wedge, sandwiched between the Relay Shear Zone at the base, and the Hart Jaune Fault at the roof of the MIZ (Hynes et al. 2000).

The MIZ experienced peak metamorphism between 1050-1040 Ma, with temperatures between 800-900°C and pressures of 20 kbar (Cox et al. 2002). It was initially buried to a depth of 40-50 km due to crustal shortening during the Ottawan event, which resulted in a thickened, imbricated crustal unit (Indares et al. 2000).

Indares et al. (1998) outlines the process of MIZ extrusion (Figure 1.4). It is proposed that after the burial of the MIZ, the asthenosphere in this location rose, replacing the more competent lithosphere beneath the MIZ. This resulted in higher peak temperatures during metamorphism, thus weakening the thickened crustal unit. With the rigidity of the lithosphere reduced, the overlying thickened crust was gravitationally unstable, and thus the MIZ was extruded from the deep crust along an Archean basement ramp, through NW directed thrusting.

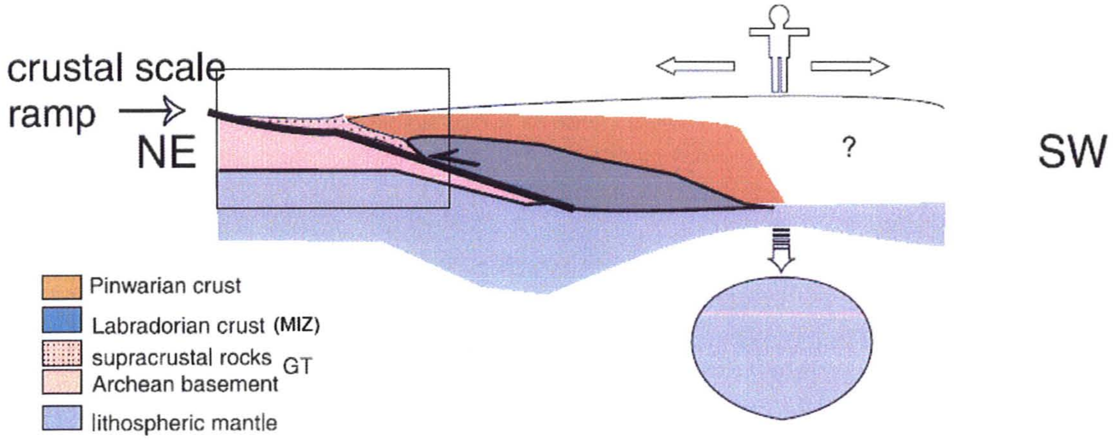

Figure 1.4: Cross section of lithosphere removal, resulting in the proposed extrusion of the MIZ. Inset box is shown in more detail in Figure 1.7 (after Indares et al. 2000)

1.2.1.3 Lelukuau Terrane

The Lelukuau Terrane is the lowest structural unit of the MIZ. It consists of a Labradorian aged anorthosite-mangerite-charnokite-granite suite (AMCG) that was imbricated into tectonic slices separated by Grenville shear zones which form a northwest directed thrust stack (Indares et al. 1998). Extensive U-Pb geochronology was completed within this terrane by Indares et al. (1998), which is summarized in Table 1.1. The three slices of this unit collectively comprise the Manicouagan Thrust System (Figure 1.5). This thrusting was initiated while the slices were deeply buried, and therefore under high pressure. In addition, the emplacement of synmetamorphic dykes around 1039 Ma marks the initiation of the MIZ extrusion. This extrusion has been modeled by Cox et al. (2002), based on evidence of rapid cooling following the peak metamorphism at 1050 Ma.

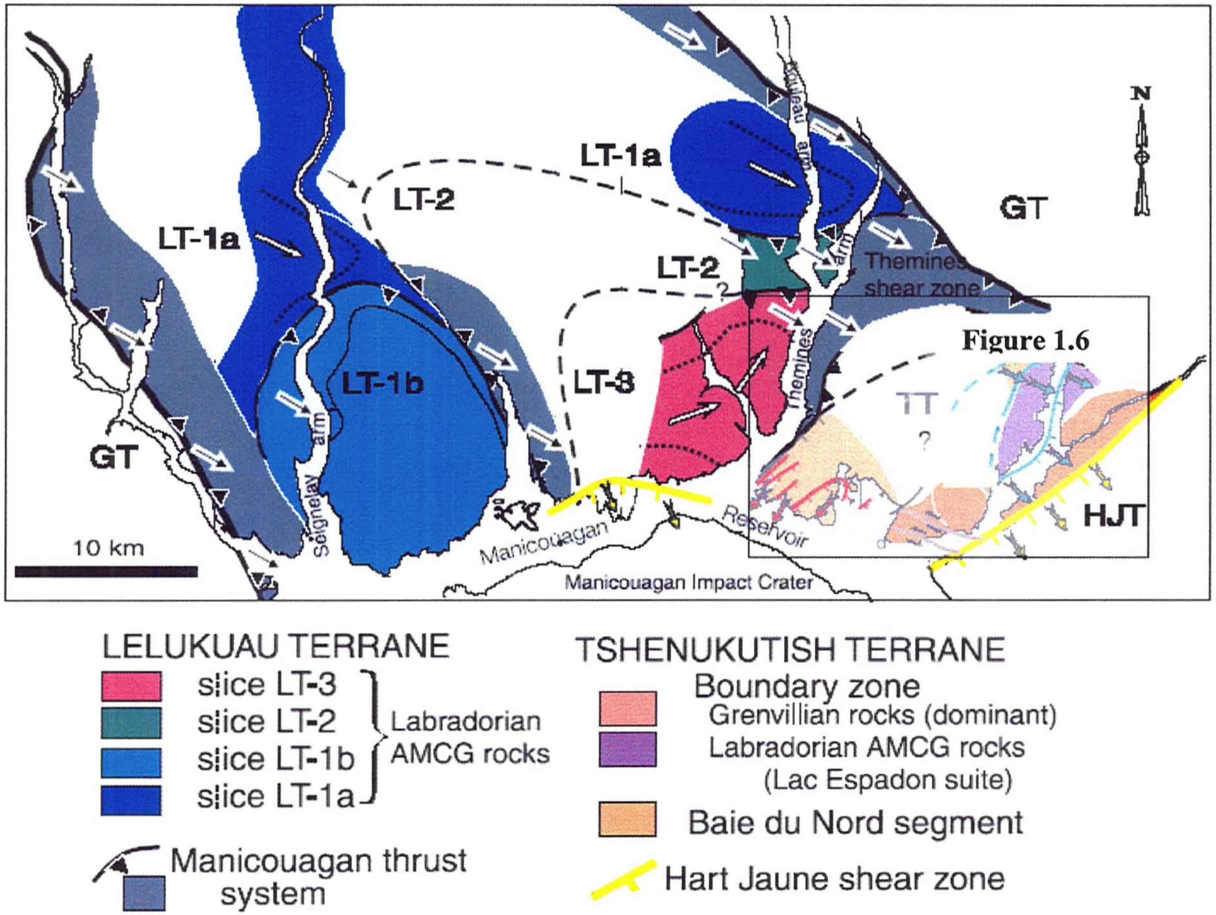

Figure 1.5: Map of the Terranes North of the Manicouagan reservoir (after Indares et al. 2000). Lelukuau Terrane (LT), Tshenukutish Terrane (TT), Gagnon Terrane (GT), Hart Jaune Terrane (HJT). The arrows indicate direction of transport. Inset is illustrated in Figure 1.6.

Table 1.1: U-Pb ages dating the Labradorian crust of the Lelukuau Terrane (after Indares et al. 1998)

Slice	Rock Type	Age Interpretation	Age
LT-1	Anorthosite	Igneous Crystallization	1692 +/-85 Ma
LT-1	Megacrystic Granite	Igneous Crystallization	1638 +15/-8 Ma
LT-3	Anorthosite	Igneous Crystallization	1628 +21/-19 Ma
LT-3	Olivine - Gabbro	Igneous Crystallization	1631 +15/-14 Ma
LT-3	Mangerite	Crystallization	1648 +11/-10 Ma
LT-3	Leucogranite	Igneous Crystallization	1300 +8/-5 Ma
LT-3	Gabbroic stock (intrusion)	Igneous Crystallization	1039 +/-2 Ma

1.2.1.4 Tshenukutish Terrane

The Tshenukutish Terrane has limited exposure, mainly located on the northeastern side of the impact structure (Figure 1.6). The majority of this terrane is believed to be located beneath the impact structure, as proposed by Hynes et al. (2000) on the basis of seismic reflective modeling, and therefore is obscured by a thick impact melt sheet. It comprises the upper thrust sheet of the MIZ, and contains two lithotectonic units: Baie du Nord Segment (BNS) and the structurally higher Boundary Zone (BZ) (Cox et al. 2002).

The tectonic evolution of the Tshenukutish Terrane is complex and is described in Figure 1.7(A-E). The BNS, which is composed of 1450 Ma Pinwarian diorite and orthogneiss (Indares et al. 1998, 2000) was thrust over the Lelukuau terrane in a NW directed thrust movement (A).

Following this, material from lower crustal levels within the buried MIZ was thrust over the BNS in an out-of-sequence thrusting event, folding the BNS in the process. This material is known as the Lac Espadon Suite of the BZ (B).

This was followed by the intrusion of Hart Jaune granite into the BZ (C2), which was dated at 1017-1007 Ma (Indares et. al. 2000), as well as SE extension along both the Espadon shear zone in the east of the Terrane(C2), and the Beaupre Shear Zone and the Brien High Strain System in the west (C1).

Finally, the Hart Jaune Terrane, which will be discussed later, was thrust over this unit at approximately 1015 Ma (Cox et al. 2002) (D). Later, SE extension occurred along the Hart Jaune Shear Zone during the Rigolet Pulse of the Grenville Orogeny, resulting in the current configuration of the MIZ and Hart Jaune Terrane (E).

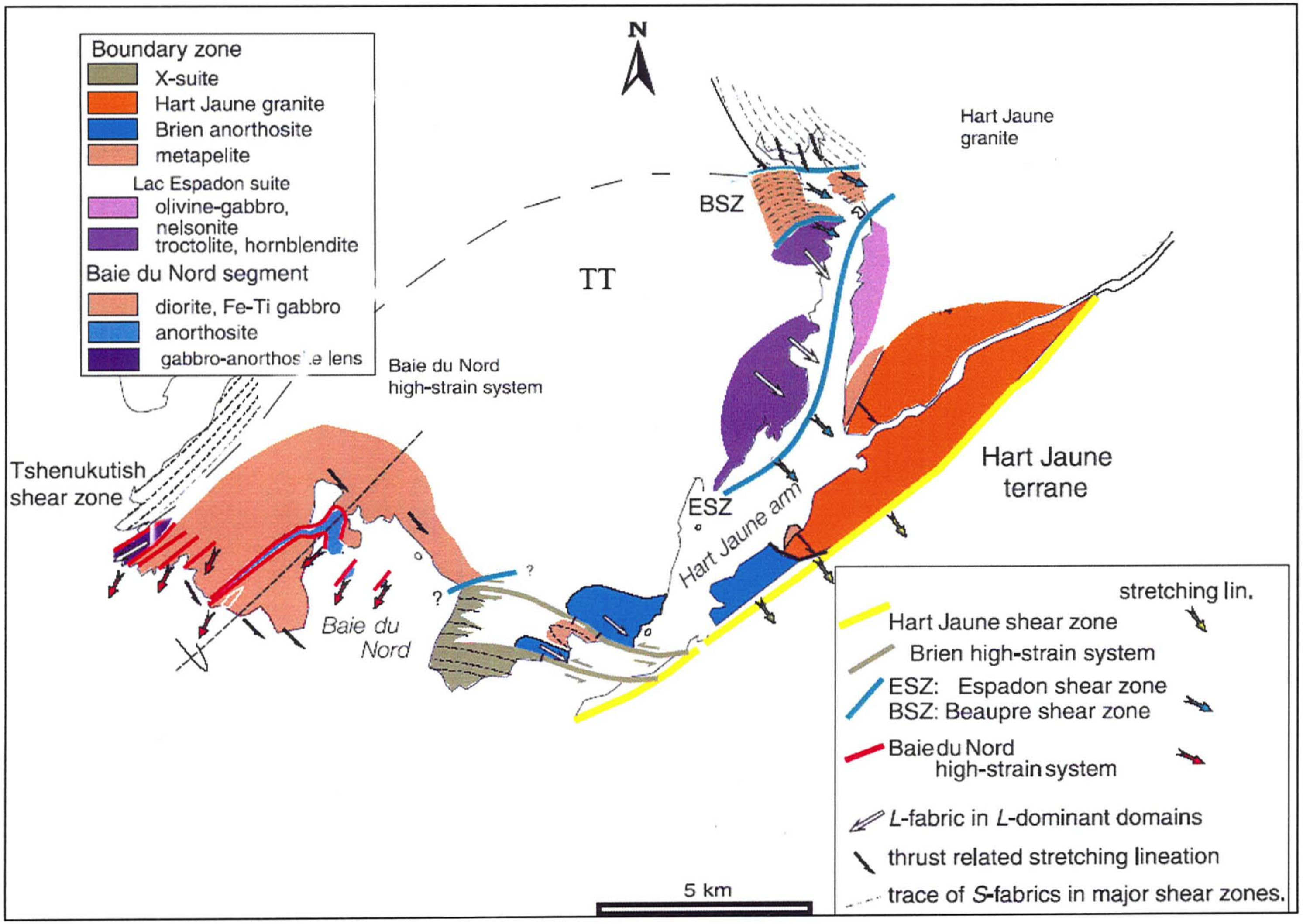

Figure 1.6: Boundary Zone and the Baie du Nord of the Tshenukutish Terrane (after Indares et al. 2000). Inset from Figure 1.5.

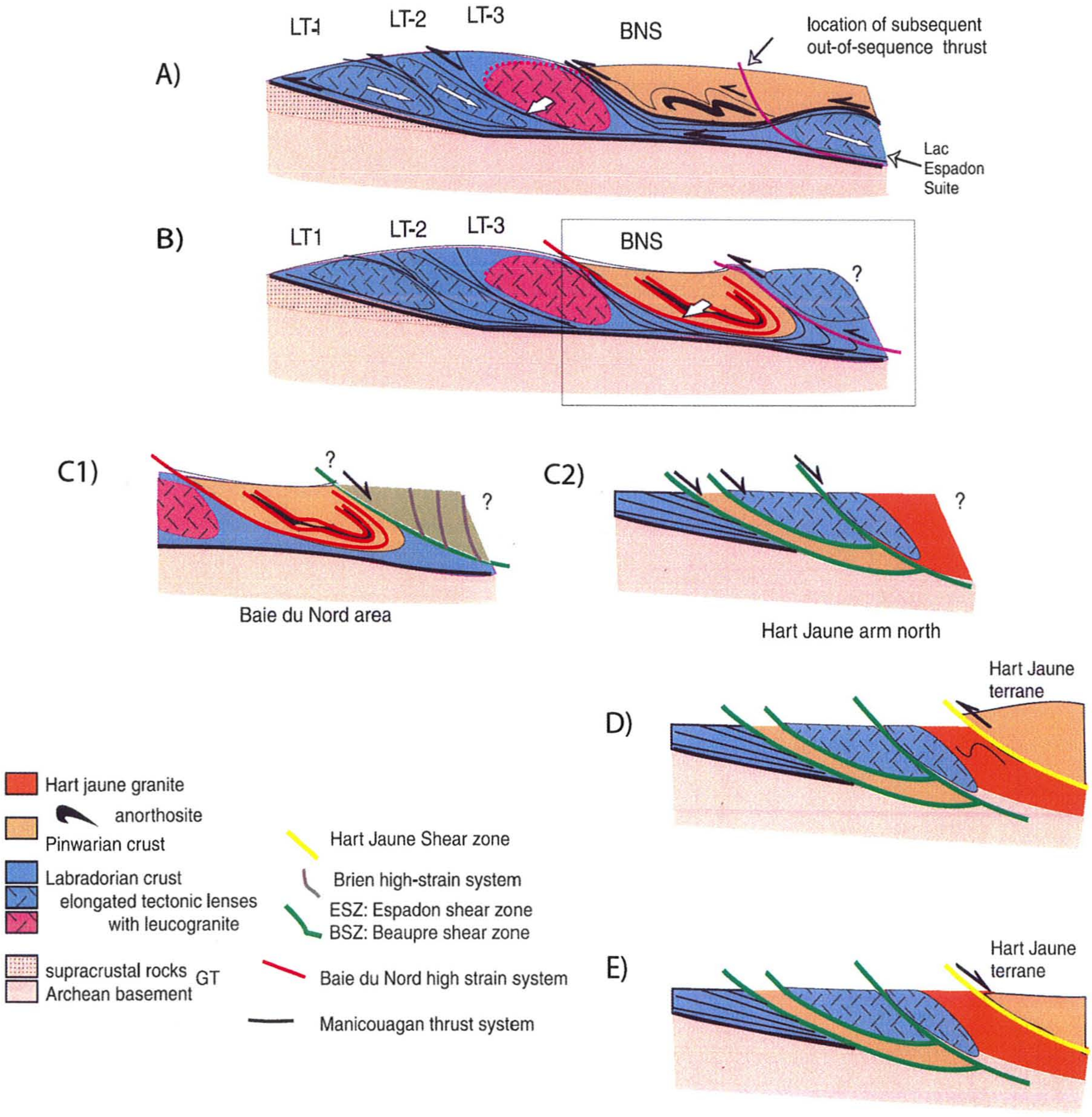

Figure 1.7: Step by step cross sections illustrating the extrusion and evolution of MIZ (after Indares et al. 2000).

1.2.1.5 Berthé Terrane

The Berthé Terrane is located to southeast of the Manicouagan reservoir. It is structurally lower than the Hart Jaune Terrane, but overlies the MIZ. This terrane contains two distinct units: Gabriel Complex and the Banded Complex (Figure 1.8). It is mainly composed of tonalitic gneiss, and the peak metamorphic temperature of this terrane has been calculated by Indares and Dunning (2004) as similar to that of the MIZ. Therefore, it is likely the Gabriel Complex was metamorphosed under similar temperature conditions as the MIZ, however, as the Gabriel Complex is a lower pressure crustal segment, it was not buried to the same depth during this metamorphism (Indares and Dunning, 2004).

The Gabriel Complex likely acted as the hanging wall during the extrusion of the MIZ to the surface. The northern extent of this terrane is described by the Gabriel Shear Zone (GaSZ) (Figure 1.3), a steeply southeast dipping – to vertical shear zone. The orientation of this shear zone is a result of prolonged crustal shortening, causing the Gabriel Complex to ride up over the synformal Hart Jaune Terrane (Indares and Dunning, 2004).

The Banded Complex refers to alternating layers of felsic and mafic layers south of, and structurally higher than the Gabriel Complex. The Banded Complex is a medium-low pressure metamorphic crustal unit, which has late Grenvillian metamorphism at approximately 996-971 Ma (Indares and Dunning, 2004).

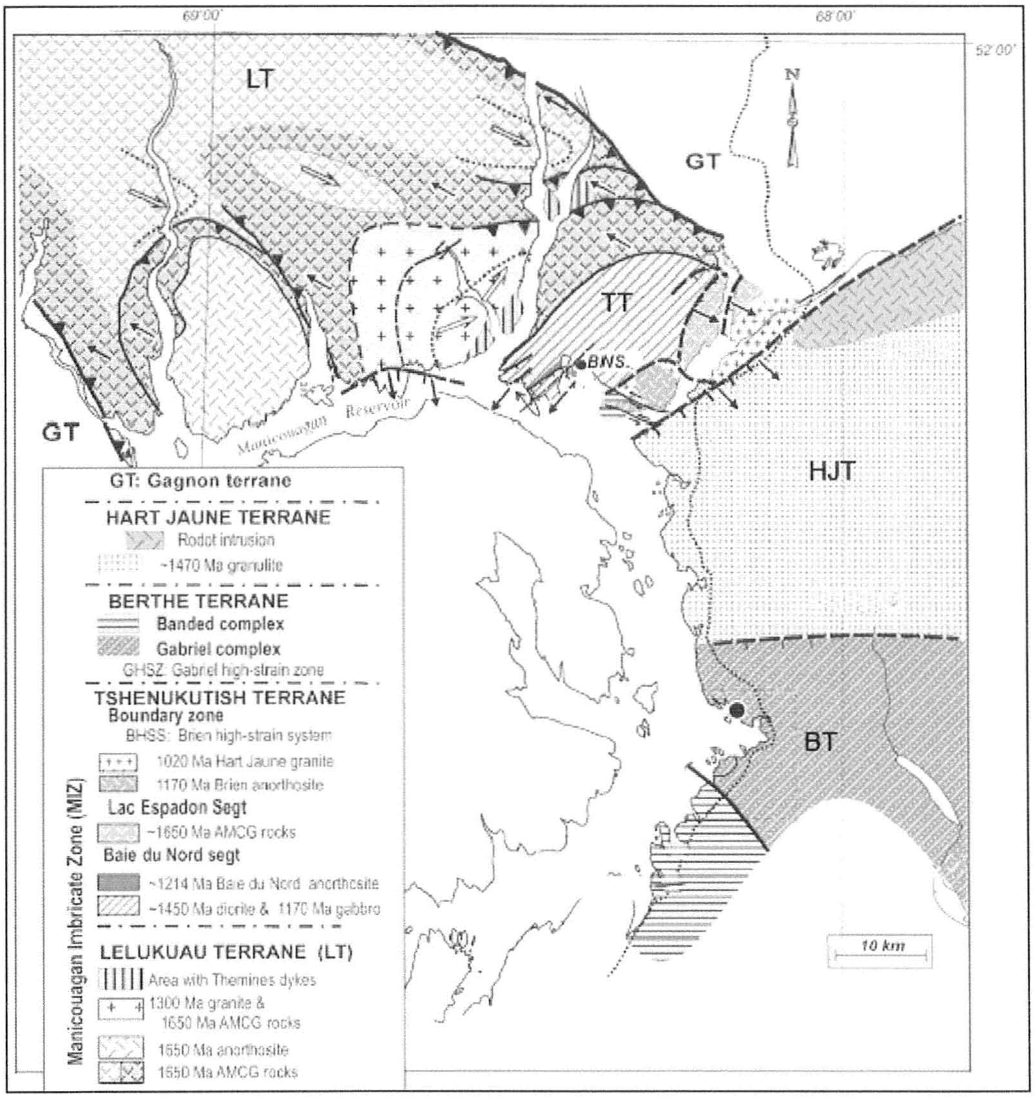

Figure 1.8: Summary of Geologic Terrane on eastern side of Manicouagan reservoir, with the location of the Gabriel Complex and Banded Complex boundary within the Berthé Terrane (after Indares and Dunning, 2004).

1.2.1.6 Hart Jaune Terrane

The Hart Jaune terrane is located on the eastern side of the reservoir. It is slightly unusual in terms of its evolutionary history as it is an erosional remnant of an allochthonous terrane composed of mafic and metasedimentary lithologies that was thrust over the Gabriel Complex of the Berthé Terrane. These mafic granulites have been dated at 1450 Ma (Indares 2000).

This terrane represents the highest structural level in the Manicouagan region, in addition to being the lowest pressure segment as well. Therefore, this terrane is the only terrane that was not an active part of the MIZ extrusion process. It was thrust over the MIZ in the north following extrusion, during the Rigolet Pulse of the Grenville Orogen. This suggests again, that crustal shortening outlasted the extrusion of the MIZ (Indares and Dunning 2004). After thrusting was completed, continued shortening caused the Hart Jaune Terrane to develop into an isoclinal syncline that was eventually over-rode by the Gabriel Complex.

1.2.2 Summary

The structure of the Manicouagan area is summarized in Figure 1.9. The lowest structural level in the Manicouagan area is the Gagnon Terrane. Above this is the MIZ, which was initially buried during crustal thickening during the Ottawan event, and experienced high pressure metamorphism. Its two components, the Lelukuau Terrane, and the structurally higher Tshenukutish Terrane were then extruded and emplaced over the Gagnon Terrane in a NW directed movement.

The Gabriel Complex of the Berthé Terrane was likely the hanging wall of the MIZ during its extrusion from deep crustal levels. It was thrust over by the Hart Jaune Terrane, which subsequently eroded to its present day size.

The Hart Jaune Terrane shows little evidence of metamorphism during the Ottawan event, and therefore it is believed that this terrane was not involved in the burial and extrusion of the MIZ, but remained at high structural levels, before being thrust over the MIZ after the Gabriel Complex, during crustal shortening.

The Banded Complex of the Berthé Terrane is the southernmost terrane. It was thrust northward over the other terranes in the area, and displays evidence of metamorphism from the Rigolet Pulse of the Grenville Orogeny. After brief periods of extension, the terranes now sit in their current configuration.

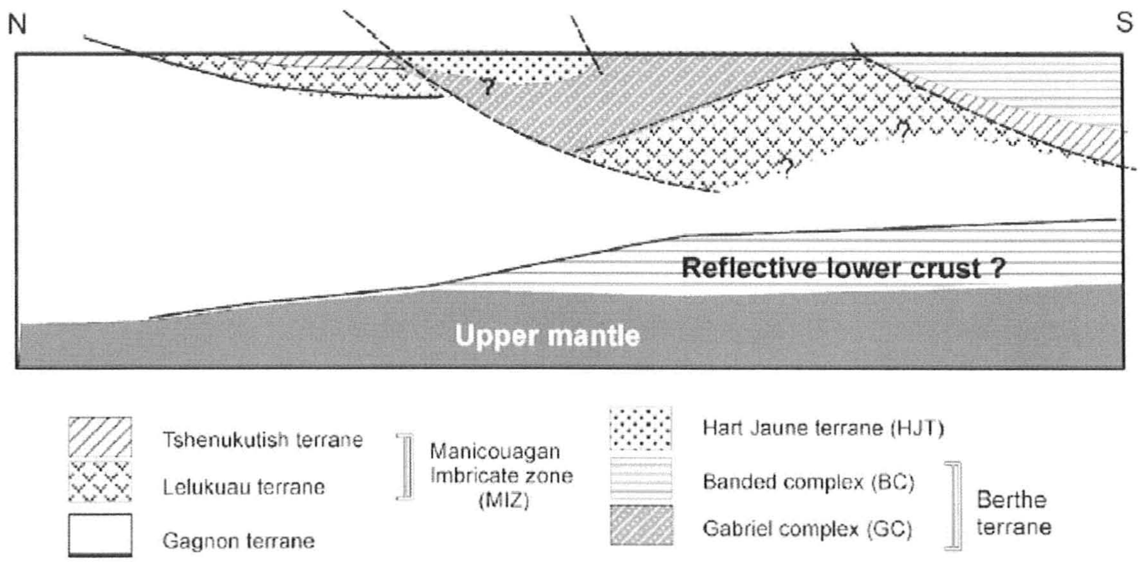

Figure 1.9: Cross section of Manicouagan Structural Terranes (Indares and Dunning, 2004)

1.3 Project Objectives

In addition to the complex underlying geology of Manicouagan, Quebec, the 214 Ma hypervelocity impact event has left the target or country rock within the impact vicinity both geologically complex and inaccessible for traditional geological analysis. By evaluating the isotopic signature of the differing crustal bodies in the area, it is possible to delineate the boundaries between the terranes as well as confine the location of the ABT through the impact structure. This can be accomplished through the analysis of samples taken from country rock beneath the impact through drill cores. Information gathered through these means should yield an accurate evolutionary history of the region based on isotopic signatures throughout the entire area, as opposed to interpolating the boundaries and evolutionary histories for those regions that are otherwise inaccessible.

CHAPTER 2: SM-ND SYSTEMS

2.0 Nd Model Ages

The time of crustal extraction from the mantle marks the protolith age, or the time of original crustal formation of a crustal terrane. Often, a crustal terrane will undergo orogenic events, where melting or metamorphism cause subsequent re-crystallization. Such a subsequent event, when calculated through means of geochronological methods such as the U-Pb system, would be known as a crystallization age of an individual pluton within the crustal terrane.

In rock assemblages that have experienced multiple orogenies, such as those found in the Grenville Province, metamorphic episodes often cause the isotopic system to become open. Transport of isotopes from their original position can occur, effectively changing the isotopic composition of geological samples, producing either erroneous results or dating the age of crystallization of a younger plutonic rock, as opposed to calculating the age of original crustal formation. This is often a limitation in such dating methods as the Rb-Sr system, the Ar-Ar system and even the U-Pb system. In contrast, the Sm-Nd system is more resistant to resetting, and thus is able to yield accurate crustal protolith ages in terranes that have undergone intense metamorphic episodes. Consequently, as Sm-Nd ages are consistent with ages found using the U-Pb or Rb-Sr methods in regions without a metamorphic overprint; they can be utilized in regions where these methods are not adequate.

^{147}Sm has a half life of 106 Byr, and therefore can produce measurable amounts of its daughter isotope neodymium (^{143}Nd) on a time scale of millions of years. This half life is equivalent to a decay constant of $6.54*10^{-12}$/year.

The decay system can be represented by the equation:

$$\left(\frac{^{143}Nd}{^{144}Nd}\right) = \left(\frac{^{143}Nd}{^{144}Nd}\right)_I + \left(\frac{^{147}Sm}{^{144}Nd}\right)(e^{\lambda t}-1)$$

The Sm-Nd model age system is based on the theory that chondritic meteorites represent the isotopic composition of the primordial solar nebula and hence the 'Bulk Earth'. Using this concept, DePaolo and Wasserburg (1976) established the Chondritic Uniform Reservoir (CHUR) which is a benchmark used to define the evolution of the isotopic composition of the earth through time.

This led to the next major development in the Sm-Nd system, which was the development of model ages, and therefore a means to calculate the time of crustal extraction from the mantle. As CHUR defines isotopic evolution of the Bulk Earth through time, measurement of the ^{143}Nd/^{144}Nd and ^{147}Sm/^{144}Nd ratios in a rock can be used to determine T_{CHUR}.

$$T_{CHUR} = \frac{1}{\lambda}\ln\left[1+\frac{\left(\frac{^{143}Nd}{^{144}Nd}\right)_{SAMPLE}-\left(\frac{^{143}Nd}{^{144}Nd}\right)_{CHUR}}{\left(\frac{^{147}Sm}{^{144}Nd}\right)_{SAMPLE}-\left(\frac{^{147}Sm}{^{144}Nd}\right)_{CHUR}}\right]$$

Therefore, by tracing the isotopic signature of a given sample back to the CHUR evolution line, the time of crustal extraction (T_{CHUR}) from a Bulk Earth reservoir can be calculated, illustrated in Figure 2.1.

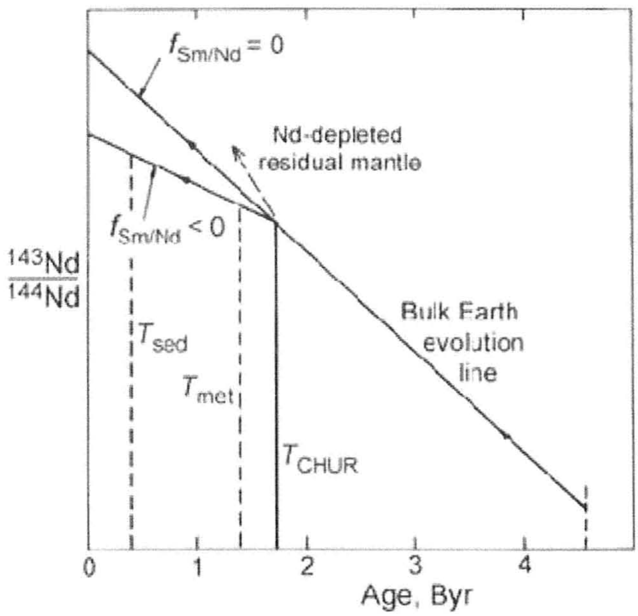

Figure 2.1: Nd Isotope evolution diagram displaying the calculation of T_{CHUR} from the CHUR evolution line (McCulloch and Wasserburg, 1978).

Around the same time, DePaolo and Wasserburg (1976a) developed the epsilon notation in order to display Nd isotope compositions. This was done in response to a variety of igneous terrestrial rock compositions plotted against time. These were remarkably consistent with the CHUR evolution line. However, since values of $^{143}Nd/^{144}Nd$ are so similar, with little to differentiate from one another and the CHUR line, epsilon notation was developed to amplify these small variations. This notation presents the value of $^{143}Nd/^{144}Nd$ in parts per 10 000 deviations from CHUR at a specific time. It allows easier comparison between initial Nd isotope ratios of different bodies.

The T_{CHUR} protolith age calculation method worked well with Archean rocks, however, younger rocks (MORB) displayed high deviations from the CHUR evolution line (Figure 2.2).

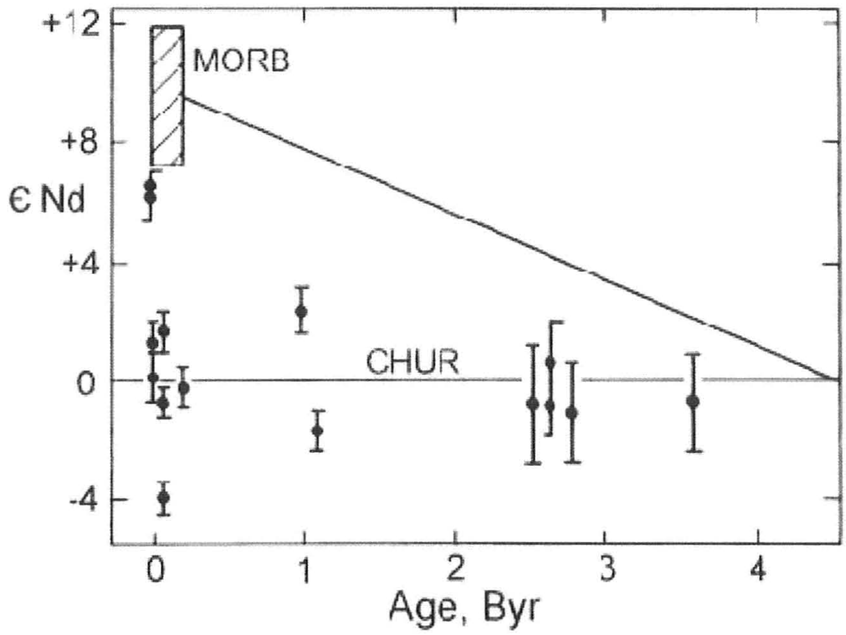

Figure 2.2: Evolution of Nd Isotopes through time represented as deviations from CHUR evolution line (DePaolo and Wasserburg, 1976a)

DePaolo (1981) proposed that this may be a consequence of progressively increasing $^{143}Nd/^{144}Nd$ ratios in the upper mantle, due to the increased Sm/Nd ratios resulting from crustal extraction through time. This gave way to the development of the depleted mantle evolution line, which is essentially a modification of the CHUR evolution line, in order to accommodate these increasing ratios and still yield accurate model ages after the Archean. This evolution line begins at CHUR, but deviates in the early Archean, gradually moving further from CHUR until it reaches present day island arc compositions. Model ages determined using this method are designated T_{DM}.

2.1 Usefulness of Nd model age calculation

The Sm-Nd technique has been tested on a variety of different rock types in a multitude of locations. By and large, the best and most reliable results have come from granitoid meta-igneous rocks. These display a high resistance to resetting, even after experiencing severe metamorphic disturbances (Dickin, 2005).

The usefulness of the Sm-Nd method in sedimentary systems is somewhat more limited. If coupled with a petrological assessment, this can yield in reliable results, calculating the provenance age of the sedimentary rock unit. However, sedimentary systems are very susceptible to contamination during both sedimentation as well as erosion, which will have a greater impact the earlier it has occurred. Because of this, it is essential to chose fresh, unweathered samples to ensure the most reliable results.

Meta-sedimentary systems are also able to produce useful results if large whole rock samples are analyzed. Various disturbances often result in open system behavior of rare earth elements (REE) on a mineral scale, therefore producing erroneous ages. Sampling the entire rock will account for the REE mobility during these disturbances and maintain original isotope ratios.

Sm-Nd model ages are generally unsuccessful in the analysis of mafic and ultra mafic meta-igneous rocks. This is due to the fact the Sm/Nd evolution lines from these rock types fall sub-parallel to the CHUR evolution line, and therefore do not yield accurate protolith ages. It does however offer information on the original Nd ratios (Dickin 2005).

2.2 Mixing in Sm-Nd Model Age Mapping

In most cases, Sm-Nd analysis will yield model ages that reflect the oldest magmatic event in the crustal history. This is usually the true crustal formation age. However, occasionally model ages are produced that do not correspond with known crustal forming events in the region. Arndt and Goldstein (1987) explain that this is likely the result Proterozoic mantle derived magmas mixed with re-melted Archean crust, producing 'mixed ages' (Figure 2.3). Therefore, it is imperative to confirm the validity of model age results with other dating method results and crustal history interpretations.

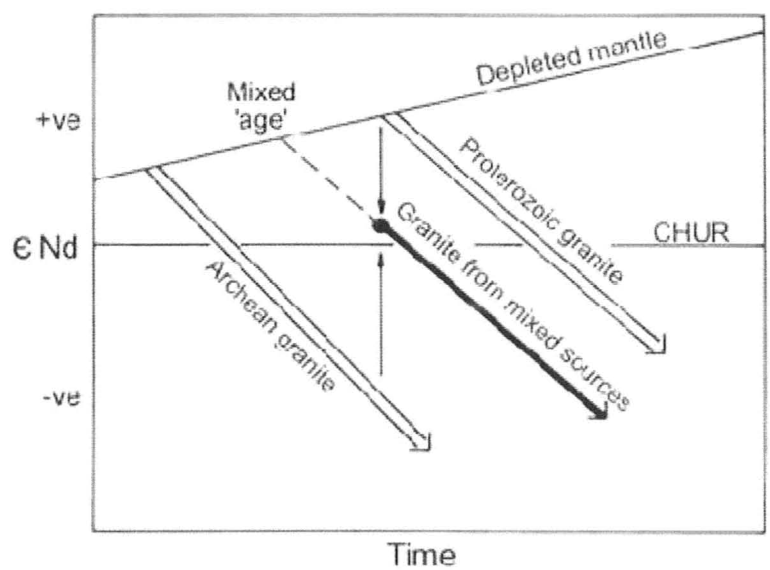

Figure 2.3: Mixed Archean and Paleoproterozoic material, resulting in erroneous 'mixed ages' reflective of both crustal sources, after Arndt and Goldstein (1987)

CHAPTER 3: RESULTS

3.0 Sampling

Samples of orthogneiss were collected from the Manicouagan Area. This included the MQ, AD, FT, CS and MA surface samples from outcrops around the impact, as well as numbered drill core samples from within the impact (Figure 3.1).

Since the ABT crosses through the Manicouagan area, the region contains a large amount of both Proterozoic and Archean aged orthogneiss. Paragneiss (Figure 3.1) however, is also found throughout the region. In the Gagnon Terrane, this manifests itself as a banded iron formation deposited on the basement gneiss. Additionally, there are pockets of anorthosite throughout the Proterozoic terranes, as well as large volumes of mafic gneiss found around the Hart Jaune Terrane. These three types of lithology; paragneiss, anorthosite and mafic gneiss, were avoided as much as possible when sampling, as these lithologies often do not yield Nd model ages representative of crustal formation.

The samples were processed at McMaster University, where they were crushed into a fine powder which is representative of the whole rock. The samples experienced several stages of chemical dissolution and element extraction, before the isotopic ratios were measured through Thermal Ionization Mass Spectrometry (TIMS). A detailed description of these methods is outlined in Appendix A.

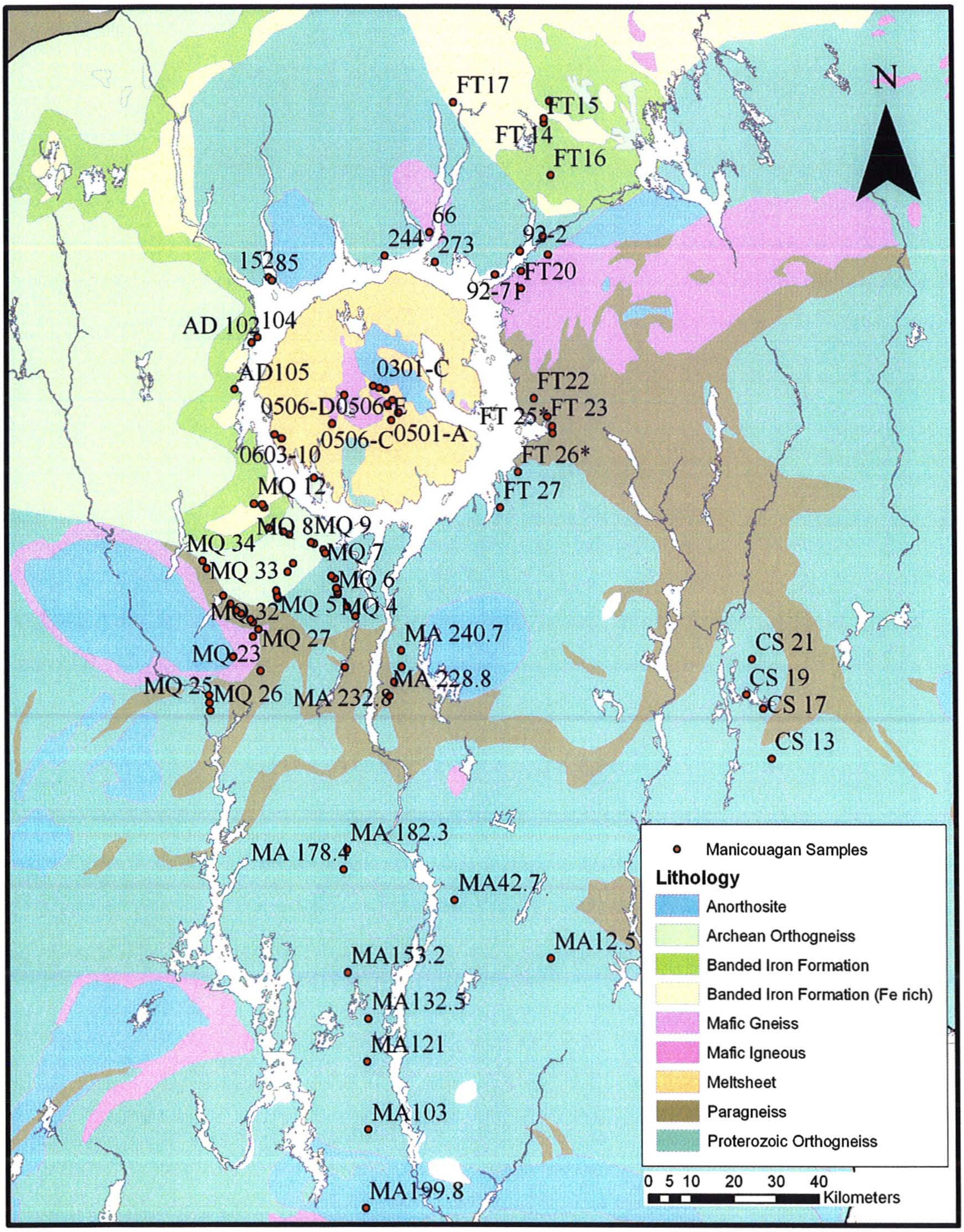

Figure 3.1: Manicouagan Sample locations with geologic map (after Davidson (comp)). Previously published samples include MA and CS datasets (Dickin, 2000).

3.1 Isotopic Ratios

Newly determined Nd isotope analyses are given in Tables 3.1-3.4, also some published data include the MA and CS samples of the Mesoproterozoic suite (Dickin, 2000). When the isotopic ratios are plotted on a Sm-Nd isochron diagram (Figure 3.2), the dataset separates into distinct sample suites, depending on their isotopic signature at the time of crustal extraction. These individual suites are defined by isochron lines, the slope of which reflects the formation age of the crustal body. Manicouagan contains three distinct crustal forming events, modeled on the isochron diagram. The first crustal body reflects Archean aged crust, and is modeled by a 2.7 Ga reference line, the second depicts Paleoproterozoic aged crust and is defined by a 1.8 Ga reference line, and the third crustal suite is Mesoproterozoic, and is modeled by a 1.5 Ga reference line. Since these ratios are so closely modeled by their respective isochron reference lines, the three separate arrays are attributed to actual geologic events.

The samples taken from the MIZ, represented as open triangles in Figure 3.2, do not fit an isochron reference line. This is owing to the larger than usual scatter of the suite, as well as a slope whose resulting age would not reflect an appropriate time frame. It is likely due to the fact that this crustal body has experienced a mixing of sources of different ages. These sources are interpreted as Archean crust mixed with large amounts of younger Paleoproterozoic magma. This magma has been characterized by several U-Pb determinations throughout the Lelukuau terrane as Labradorian aged (Table 1.1). It is reasonable then that the samples fall between the Paleoproterozoic and the Archean isochrons.

The mixing is also apparent in the Archean suite. The four Archean samples which lie farther above the isochron than the rest of the suite are also attributed to mixed crustal sources. These samples are all located very close to the ABT boundary, and are considered to have undergone some degree of crustal mixing. However, these samples still maintain a primarily Archean crustal signature, and therefore remain included within the Archean sample suite.

Table 3.1: Nd Isotope analysis on Archean samples from Manicouagan area.

	Easting	Northing	Nd ppm	Sm ppm	147Sm/144Nd	143Nd/144Nd	TDM (Ga)
Archean							
MQ 4	510 970	5 646 752	15.8	2.86	0.1096	0.511161	2.85
MQ 5	510 710	5 647 591	14.5	1.86	0.0774	0.510649	2.69
MQ 6	510 327	5 649 818	13.7	2.09	0.0922	0.510757	2.89
MQ 9	504 816	5 658 291	5.9	0.85	0.0860	0.510835	2.65
MQ 11	495 082	5 661 754	11.8	1.93	0.0989	0.510993	2.74
MQ 12	491 449	5 667 444	63.9	12.05	0.1140	0.511275	2.73
MQ 16	496 834	5 646 102	10.4	2.36	0.1371	0.511621	2.86
MQ 18	500 646	5 653 412	40.2	7.00	0.1052	0.511082	2.78
MQ 33	480 321	5 652 265	3.1	0.52	0.0992	0.511075	2.64
MQ 34	479 316	5 654 045	10.8	1.95	0.1091	0.511087	2.88
FT 13	561 000	5 761 600	26.9	4.12	0.0925	0.510893	2.72
FT 14	559 700	5 757 500	41.8	7.54	0.1089	0.511207	2.69
AD 102	491 000	5 705 000	10.0	1.40	0.0851	0.510684	2.82
AD105	487 000	5 694 000	11.0	1.60	0.0880	0.510773	2.77
FT 15	559 700	5 756 800	26.5	4.42	0.1008	0.510969	2.83
FT 16	561 300	5 744 400	24.6	4.27	0.1049	0.511087	2.76
FT 17	561 500	5 738 500	24.9	4.76	0.1156	0.511302	2.73
MQ 3	511 057	5 646 151	35.6	6.32	0.1074	0.511429	2.32
0513-11	496 359	5 683 606	17.7	3.56	0.1214	0.511538	2.57
0509-A	505 634	5 673 483	36.6	6.75	0.1115	0.511503	2.30
MQ 30	488 389	5 641 594	55.0	9.60	0.1055	0.511295	2.47
MEAN			**20.9**	**3.62**	**0.1033**	**0.511026**	**2.70**
WEIGHTED MEAN					**0.1046**	**0.511086**	
ST. DEV			**15.7**	**2.96**	**0.0137**	**0.000251**	**0.16**
2*ST. ERR			**7.6**	**1.4**	**0.0058**	**0.000107**	

Table 3.2: Nd Isotope analysis on Paleoproterozoic samples from Manicouagan area.

	Easting	Northing	Nd ppm	Sm ppm	147Sm/144Nd	143Nd/144Nd	TDM (Ga)
Paleoproterozoic							
MQ 1	515 211	5 641 038	16.2	2.21	0.0825	0.511573	1.71
MQ 2	513 320	5 643 250	61.2	10.41	0.1028	0.511623	1.84
MQ 20	491 151	5 636 244	58.5	12.56	0.1297	0.512025	1.85
MQ 25	480 885	5 620 599	35.4	7.63	0.1302	0.512018	1.87
MQ 27	492 459	5 637 894	4.5	1.06	0.1412	0.512184	1.80
MQ 29	490 673	5 640 213	31.2	4.78	0.0927	0.511490	1.96
MQ 31	487 268	5 642 410	8.8	1.71	0.1173	0.511792	1.98
FT 18	606 256	5 725 600	25.8	5.13	0.1201	0.511917	1.83
FT 19	542 217	5 721 700	24.5	4.06	0.1002	0.511682	1.83
FT 20	553 400	5 717 850	5.4	1.44	0.1604	0.512314	2.08
FT 22	556 700	5 792 000	19.8	4.04	0.1233	0.511930	1.86
FT 23	560 300	5 687 600	29.4	5.87	0.1204	0.511941	1.80
FT 24	561 500	5 685 300	59.6	8.84	0.0897	0.511576	1.80
FT 25	561 600	5 683 600	12.3	2.06	0.1009	0.511685	1.83
FT 26	553 400	5 674 600	41.3	6.85	0.1003	0.511577	1.97
FT 27	549 200	5 666 300	18.5	3.20	0.1043	0.511722	1.84
MA 240.7	526 000	5 632 700	38.4	5.43	0.0842	0.511465	1.86
MA 236.6	526 100	5 628 800	35.4	5.38	0.0920	0.511622	1.78
MA 232.8	524 300	5 625 300	68.8	13.27	0.1166	0.511846	1.88
MA 228.8	523 100	5 621 900	10.5	2.19	0.1256	0.511912	1.96
MEAN					**0.1117**	**0.511795**	**1.86**
WEIGHTED MEAN					**0.1129**	**0.511707**	
ST. DEV					**0.0197**	**0.000227**	**0.08**
2*ST. ERR					**0.0088**	**0.0001**	

Table 3.3: Nd Isotope analysis on MIZ samples from the Manicouagan area.

	Easting	Northing	Nd ppm	Sm ppm	147Sm/144Nd	143Nd/144Nd	TDM (Ga)
Manicouagan Imbricate Zone							
0502-09	520 880	5 694 490	23.5	4.21	0.1083	0.511580	2.12
0511-30	522 506	5 694 037	1.9	0.37	0.1187	0.511789	2.01
0511-31	522 506	5 694 037	16.0	2.99	0.1131	0.511742	1.97
0302-11	524 083	5 691 570	30.1	7.11	0.1429	0.512048	2.15
MA223	522 300	5 615 800	23.0	4.45	0.1167	0.511699	2.11
92ad71	548 051	5 721 104	25.3	5.15	0.1233	0.511843	2.02
AD 92.2	553 932	5 726 568	28.0	5.40	0.1164	0.511699	2.11
AD244	522 335	5 725 530	56.8	10.43	0.1111	0.511668	2.04
AD85	495 760	5 719 820	48.0	8.15	0.1026	0.511641	1.92
AD66	532 823	5 730 993	57.1	8.55	0.0905	0.511396	2.04
0301-A	519 588	5 694 978	7.1	0.99	0.0845	0.511454	1.87
0301-B	519 589	5 694 979	26.4	5.25	0.1201	0.511718	2.16
0301-C	519 590	5 694 980	25.4	4.81	0.1145	0.511731	2.02
0302-A	524 083	5 691 570	36.1	6.65	0.1112	0.511676	2.03
0501-A	523 722	5 686 894	3.8	0.84	0.1326	0.512087	1.79
0506-A	509 940	5 686 130	36.6	7.81	0.1289	0.511881	2.09
0506-B	510 940	6 686 130	33.3	5.83	0.1056	0.511619	2.03
0506-C	511 940	7 686 130	28.5	5.04	0.1067	0.511663	1.96
0506-D	512 940	8 686 130	26.2	4.52	0.1044	0.511599	2.01
0506-E	513 940	9 686 130	19.6	3.12	0.0963	0.511589	1.89
0511-A	522 506	5 694 037	9.4	2.10	0.1344	0.512038	1.95
0511-B	523 506	6 694 037	1.3	0.24	0.1120	0.511688	2.03
0511-C	524 506	7 694 037	1.6	0.28	0.1081	0.511758	1.87
0602-A	512 647	5 692 881	12.4	2.62	0.1277	0.511814	2.20
0602-B	512 648	5 692 882	23.8	5.07	0.1286	0.511888	2.07
0602-C	512 649	5 692 883	35.7	6.12	0.1038	0.511588	2.03
0602-D	512 650	5 692 884	24.8	4.96	0.1211	0.511833	2.01
0608-A	522 850	5 690 601	26.4	4.75	0.1088	0.511671	1.99
0608-B	522 851	5 690 602	39.7	7.75	0.1180	0.511783	2.01
0608-C	522 852	5 690 603	24.2	4.50	0.1121	0.511715	1.99
0608-D	522 853	5 690 604	20.1	4.84	0.1457	0.512103	2.11
MEAN			**24.9**	**4.67**	**0.1152**	**0.511742**	**2.02**
WEIGHTED MEAN					**0.1129**	**0.511707**	
ST. DEV			**14.4**	**2.56**	**0.0138**	**0.000168**	**0.09**
2*ST.ERR			**5.2**		**0.0050**	**0.000060**	

Table 3.4: Nd Isotope analysis on Mesoproterozoic samples taken from Dickin and McNutt (2000)

	Easting	Northing	Nd ppm	Sm ppm	147Sm/144Nd	143Nd/144Nd	TDM (Ga)
Mesoproterozoic							
MA178.4	512 200	5 581 200	28.6	5.20	0.1100	0.511981	1.56
MA182.3	513 100	5 585 900	41.3	7.45	0.1089	0.511964	1.57
CS13	612 700	5 607 300	19.06	4.05	0.1285	0.512146	1.60
CS17	610 800	5 619 000	39.9	7.21	0.1092	0.511951	1.59
CS19	606 800	5 622 300	19.1	4.11	0.1299	0.512168	1.59
CS21	608 200	5 630 700	27.3	5.07	0.1122	0.511975	1.60
92ad98	599 359	5 730 154	74.1	15.85	0.1294	0.512089	1.72
MA12.5	552 300	5 560 700	4.4	0.85	0.1167	0.512045	1.57
MA103	517 900	5 520 500	45.4	9.32	0.1241	0.512116	1.57
MA121	517 700	5 536 400	16.1	3.01	0.1131	0.512016	1.55
MA132.5	518 000	5 546 400	39.5	8.60	0.1315	0.512197	1.56
MA153.2	513 200	5 557 300	4.1	0.71	0.1048	0.511930	1.56
MA199	517 300	5 502 200	16.9	3.41	0.1217	0.512097	1.56
MEAN						**0.512052**	**1.58**
ST. DEV						**0.000089**	**0.04**

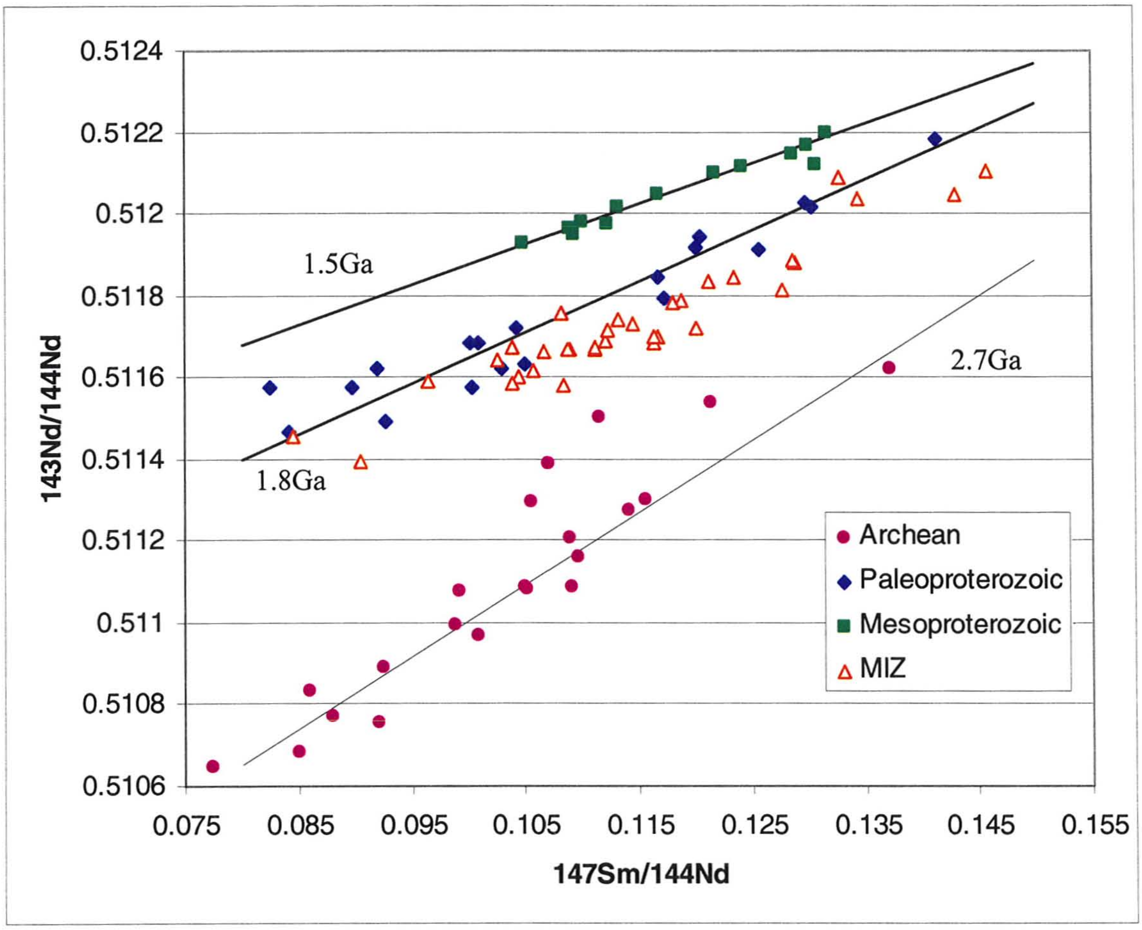

Figure 3.2: Sm-Nd isochron diagram displaying 3 distinct crustal forming events in Manicouagan, Quebec.

3.2 Age frequency

A frequency distribution of T_{DM} model ages calculated for Manicouagan display three peaks in the crustal ages. This again supports three distinct crustal bodies (Figure 3.3). The Archean peak is found at 2.7 Ga, the Paleoproterozoic peak is at 1.8 Ga, and the Mesoproterozoic peak is indicated at 1.5 Ga, which correspond with the reference lines from the isochron diagram in Figure 3.2. In contrast, the ages calculated from the MIZ display a wide range in ages from 1.7 Ga to 2.2 Ga.

The same pattern is displayed through modeling the frequency of the epsilon values calculated within the Manicouagan crustal terranes for 1.65Ga. The wide range modeled by the MIZ is attributed to a mixing of Paleoproterozoic material with older Archean crust. As this mixing is present in some Archean samples as well, this accounts for the tail on the left of the Archean age peak on both frequency diagrams.

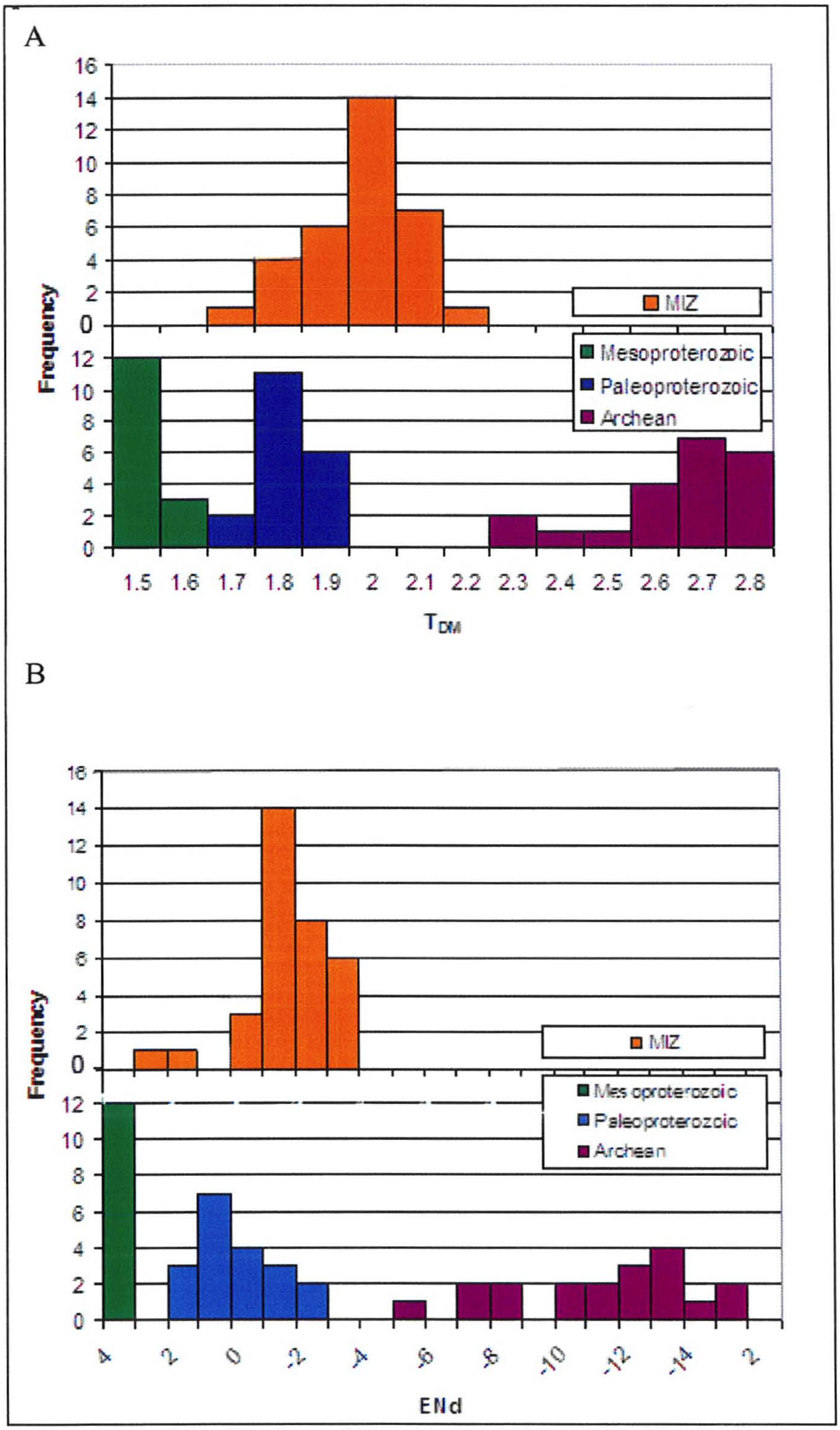

Figure 3.3: Frequency Distribution of T_{DM} Ages (A) and Epsilon Nd values (B) for the Manicouagan samples.

3.3 Geological Distribution of Age Results

The distribution of the Nd model ages is spatially illustrated in Figure 3.4, where the Mesoproterozoic terrane is confined to the southeast, the Paleoproterozoic crust is located through the center of the study area and the Archean is found in the northwest. This younging-to-the-southeast distribution follows a trend that is present throughout much of the Grenville Province, in roughly sub-parallel northeast trending crustal belts. The mixed MIZ ages are found sandwiched between the Archean and Paleoproterozoic crustal terranes, and do not follow this sub-parallel belted pattern. Instead the MIZ encompasses most of the area beneath the impact and extends north of the impact structure.

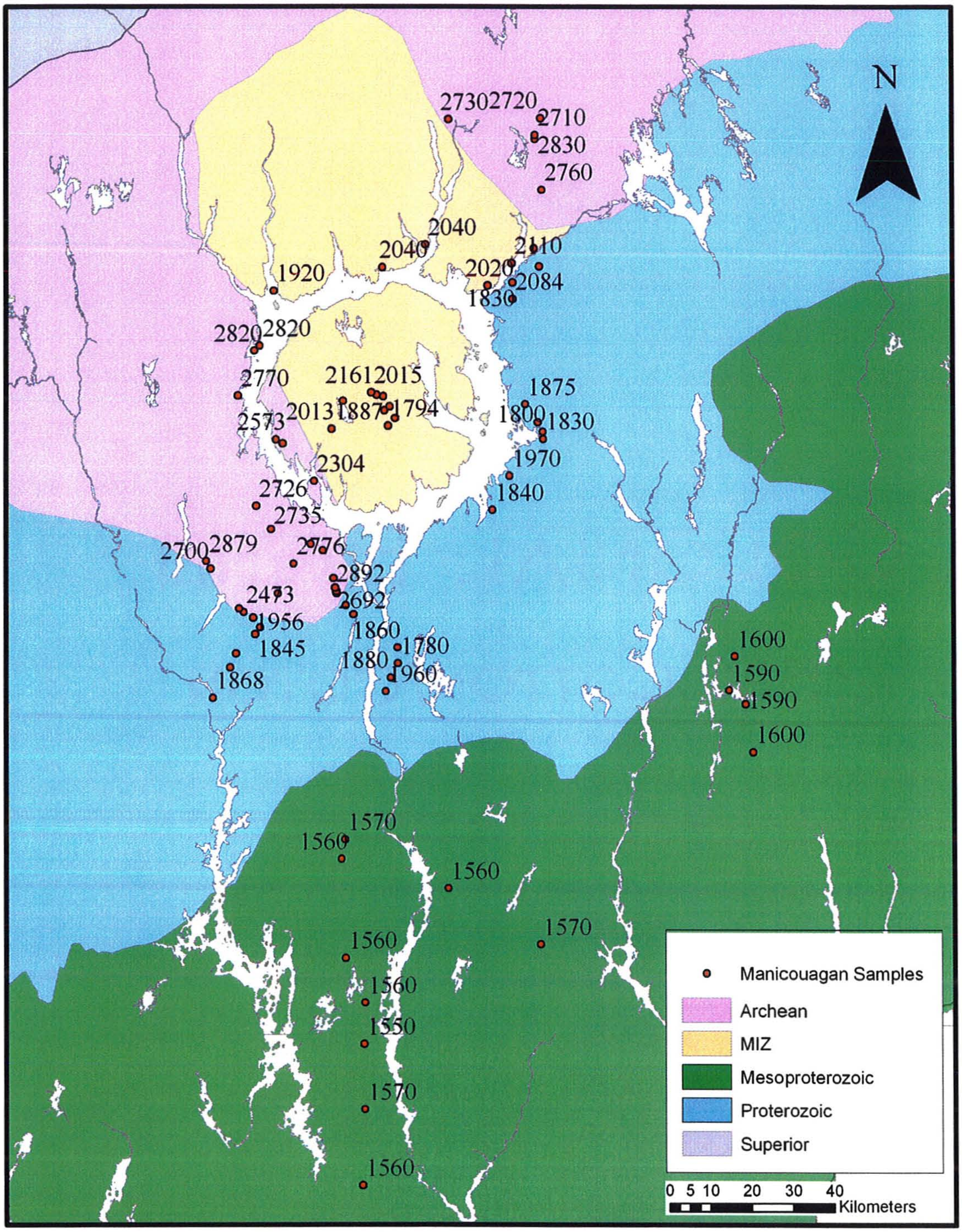

Figure 3.4: Crustal terranes as defined model age map of Manicouagan, Quebec. (NTDB, 2006)

3.4 Nd Concentration

As a means of comparing the isotopic composition of the differing crustal suites in the area, an epsilon Nd diagram was constructed with respect to the Nd concentration. The time frame for which the epsilon values were calculated was 1.65 Ga, as it corroborates with U-Pb ages found in several of the terranes. Moreover, since the Lelukuau Terrane has been extensively dated as Labradorian aged, it is likely that this is the time of the mixing event in the MIZ. Figure 3.5 illustrates that the Proterozoic crustal terrane has the highest epsilon values, while the Archean terrane consists of the lowest epsilon values of the crustal bodies. The MIZ displays epsilon values that are similar to the Paleoproterozoic terrane, but are slightly lower throughout the entire suite. This is expected of a crustal body that is likely Paleoproterozoic in age, but has been contaminated by Archean aged material.

The Archean suite, which is possibly the most distinctive, again displays evidence of mixing. This is apparent in the samples that are found on the Archean – MIZ/Paleoproterozoic boundary with slightly younger ages than the rest of the terrane. These correspond to the samples with the highest epsilon values in Figure 3.5. This is again typical for a mixed Paleoproterozoic –Archean crustal signature that contains more Archean material than the rest of the mixed crust and therefore an epsilon value higher than the rest of the pristine Archean crustal suite, but still lower than the mixed MIZ crustal suite. Since these samples still display the same scatter as the rest of the Archean suite, they have remained classified as Archean derived crust.

Since the MIZ is a result of crustal mixing with mantle derived magma, it can be modeled by a simple two component mixing model. In order to do this, the isotopic composition of both materials as well as the Nd concentration of each material involved in the mixing must be considered. Therefore, at least two measured variables must be involved in this calculation. The measured variables used in this case are isotopic ratios and elemental abundances, or $^{143}Nd/^{144}Nd$ ratios, and Nd concentration.

The timing of the mixing event has been constrained to approximately 1.65 Ga by U-Pb evidence (Table 1.1), and therefore the process can be modeled in Figure 3.5 at this time. The mixing line demonstrates the theoretical average value of the isotopic signature beginning with 100% Archean, modeled by the Archean suite mean, and becoming increasingly contaminated with Proterozoic material, until the mixture approaches 100% Proterozoic material at the Proterozoic suite mean. The epsilon value at which the MIZ suite mean intersects the mixing line would yield information on the amount of each end member involved.

Figure 3.5 demonstrates that the crustal signature present in the MIZ represents approximately 80% Paleoproterozoic crust with 20% Archean material. In addition, the mixed crustal source explanation fits well with previous studies in the area, as there is no evidence for localized crustal formation at 2.0 Ga.

Although the isotopic ratios have little associated error, there is some error associated with the absolute values calculated from the samples, such as the elemental concentration. This is demonstrated through the error bars, which identify two standard errors on each mean. It is likely that this is the reason that the MIZ mean does not fall directly on the Paleoproterozoic-Archean mixing line. Since the error bars overlap, it is reasonable to assume that the mixing model is valid.

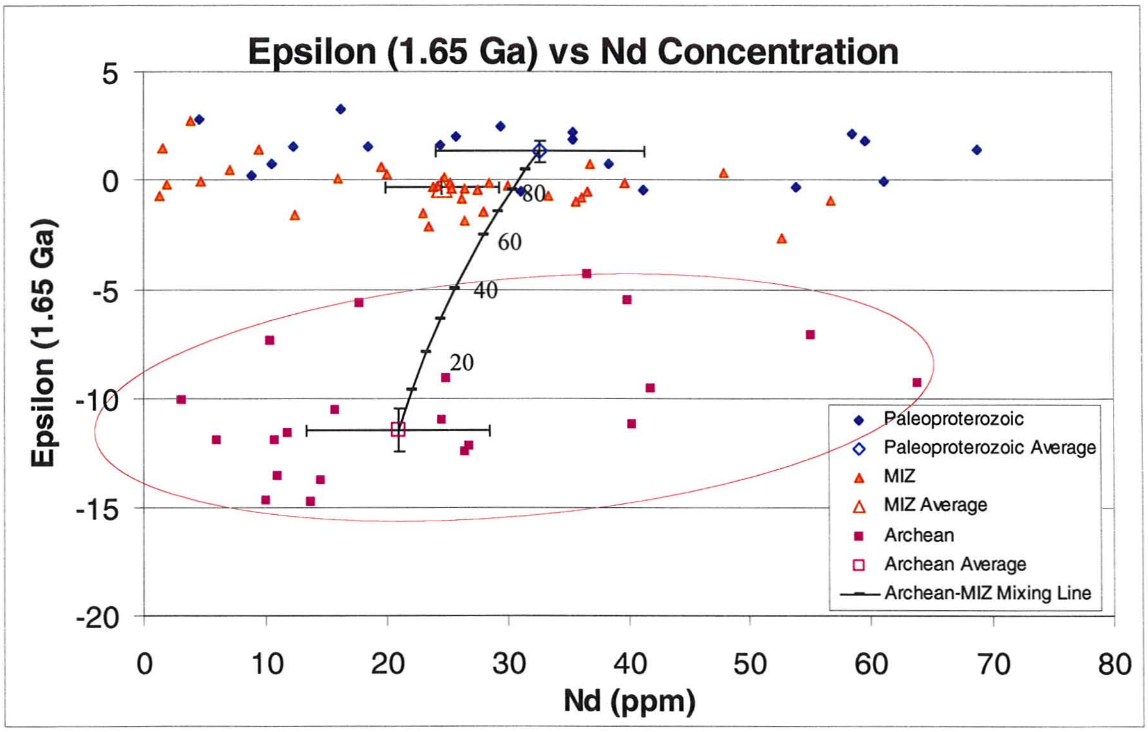

Figure 3.5: Plot of Epsilon Nd (1.65Ga) versus Nd Concentration. Amount of Paleoproterozoic material involved in MIZ crustal composition marked as percentages along the mixing line.

3.5 Major Element Analysis

In order to obtain a more complete understanding of the petrochemistry of the crust in each terrane, major elemental analysis was performed on the dated samples. This geochemical analysis was completed at Activation Laboratories, and the results were analyzed based on the Debon and LeFort (1983) Q-P chemical –mineralogical classification scheme. This classification defines the magmatic association of granitoid suites.

The quartz and plagioclase compositions are modeled in Figure 3.6 by:

$$\mathbf{Q = Si/3 - (K + Na + 2Ca/3) \quad and \quad P = K - (Na + Ca)}$$

This method classifies the individual samples into a lithologic category in order to define individual sample characteristics. These are: granite (gr), granodiorite(gd), tonalite (tn), adamellite(ad), monzonite(mz), quartz syenite(qs), quartz monzonite(qmz), quartz monzodiorite(qmd), quartz diorite(qd), syenite(sy), monzodiorite(md), diorite-anorthosite(di). Following this, the magmatic association of each crustal suite is determined with regards to the relative alkalinity of the suite as a whole (Debon and LeFort, 1983).

The difference between the associations reflects the evolution of the alkali content throughout the suite, distinguishing samples that are composed predominantly of juvenile mantle derived material from samples which result from the anatexis of pre-existing sialic material.

The juvenile crustal derivatives are represented in Figure 3.6 ranging from diorite, quartz-diorite, tonalite, granodiorite, and adamellite, whereas the more alkaline samples, reflective of anatexis evolve through the quartzmonzodiroite, granodiorite and adamellite fields. This occurs as a result of more prolonged magmatic differentiation which leads to a more alkali-rich composition. This is consistent with our findings in the Manicouagan region, where the Mesoproterozoic, Paleoproterozoic and Archean samples predominantly fall within the juvenile crustal signature fields. The MIZ evolves through the middle of the QP-diagram, supporting the mixed source theory.

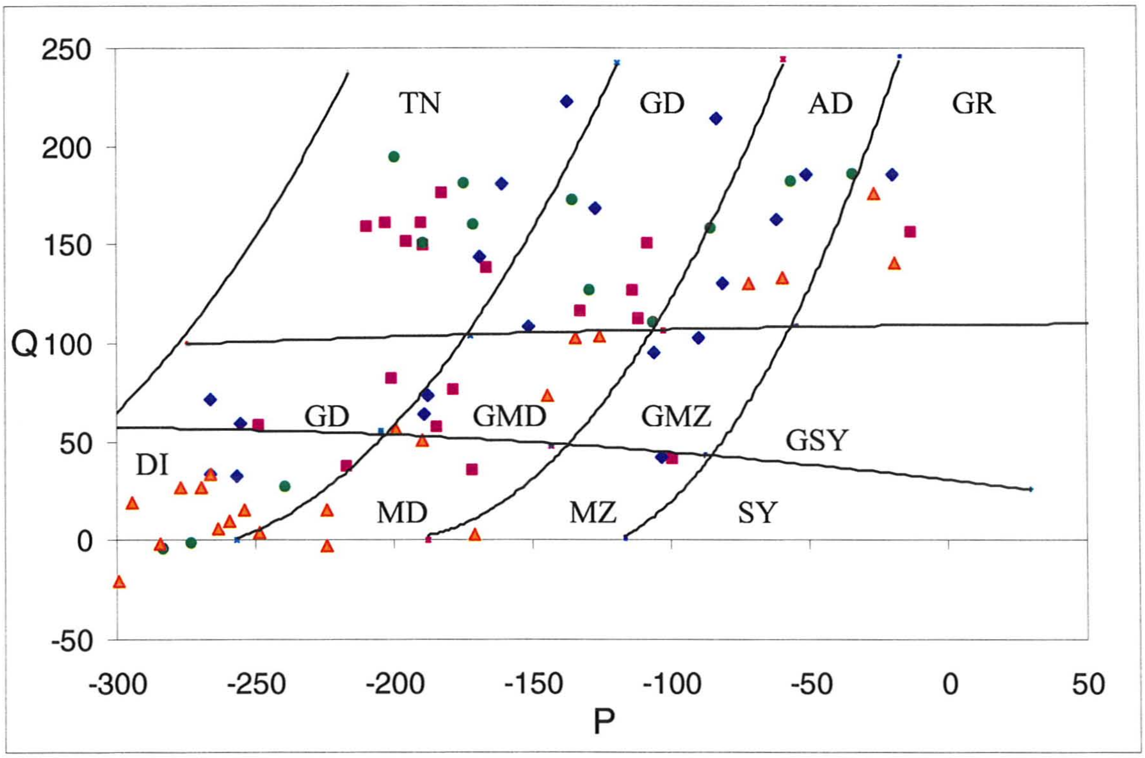

Figure 3.6: Petrogenic Quartz-Plagioclase grid (after Debon and LeFort, 1983).

CHAPTER 4: DISCUSSION

4.1 Location of the ABT

Since the melt sheet material covers two thirds of the impact crater, the location of the ABT is buried beneath it. The use of drill core in this area has enabled the analysis of country rock below the melt material and made crustal differentiation possible. Although all of the drill core samples produced a mixed isotopic signature, the amount of Archean material in each sample was drastically different. The ages found in the west side of the island reflect a crustal composition that contains significantly more Archean material, producing T_{DM} ages ranging from 2.3-2.5 Ga. The samples found in the center of the island reflect crustal material with a much higher Paleoproterozoic content, and produced ages around 2.0 Ga. Therefore, the location of the ABT within the impact structure has been confined between these two sets of crustal signatures (Figure 4.1).

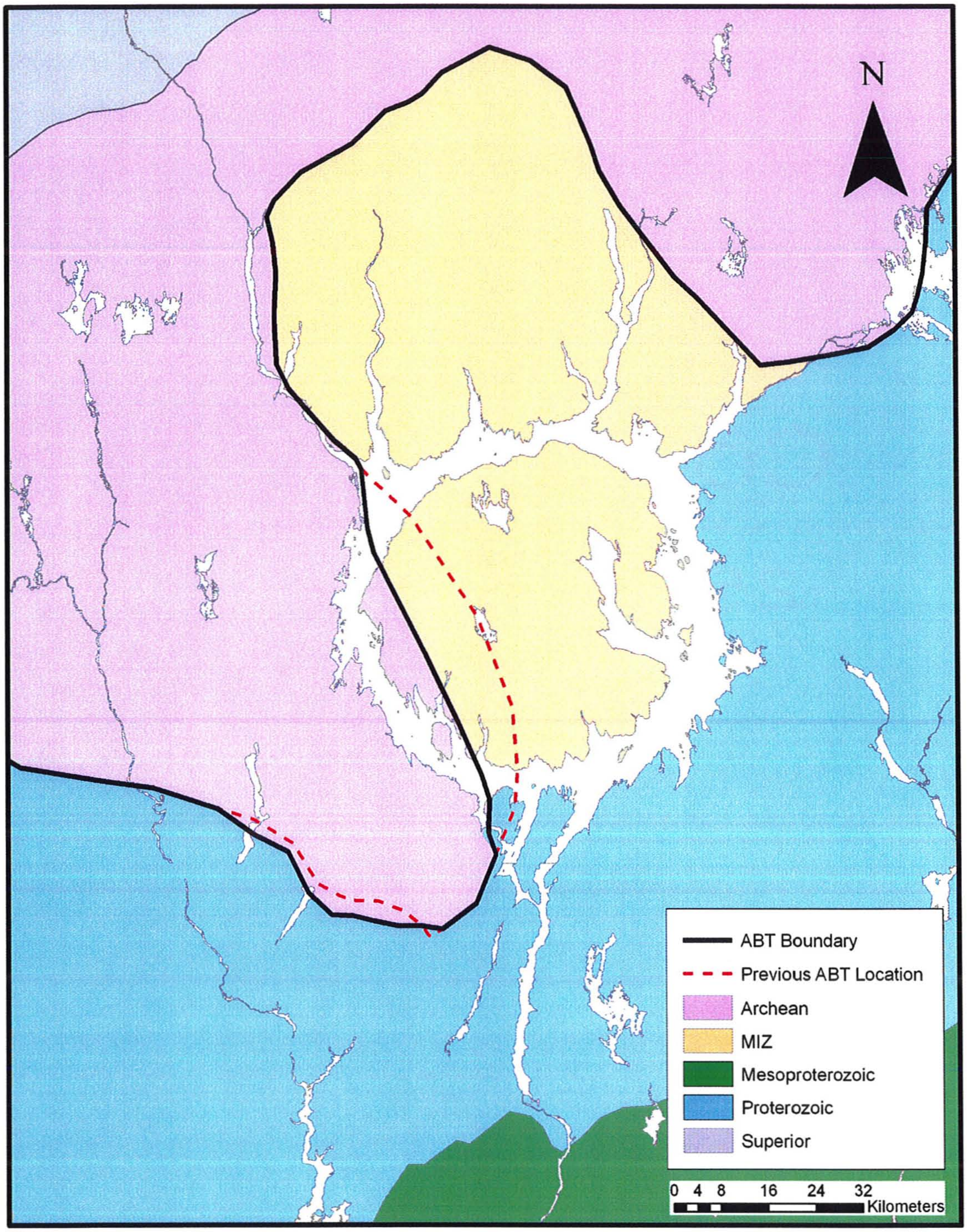

Figure 4.1: Location of the ABT within the Manicouagan impact crater. (source: NTDB, 2006)

4.2 Terrane Differentiation

As mentioned earlier, the boundaries between the Lelukuau and Tshenukutish terranes have been obscured as a result of the Impact structure. However, differences in the isotopic signatures between these two terranes may delineate the boundary between them. This analysis is made possible through the use of drill cores, as these allow access to the country rock beneath the melt sheet. A comparison of the isotopic signature of the Lelukuau and Tshenukutish terranes is demonstrated in Figure 4.2. This is based on their proposed boundaries modeled by Lithoprobe line 55 (Hynes et al. 2000). Here we see that the two terranes have produced similar T_{DM} ages at approximately the same frequency. As a result, it is likely that the two terranes in fact come from the same crustal unit. It is because of this that the isotopic analysis is unable to differentiate between the two terranes, and therefore, the boundary cannot be delineated in this region.

The terranes of the Paleoproterozoic crustal body were compared also. Figure 4.3 illustrates that these terranes do display a slight bias, where the Berthé Terrane produced a higher number of younger crustal formation ages than that of the Hart Jaune Terrane. It is important to note however, that sampling in the Hart Jaune Terrane was limited, as this area is extensively composed of mafic and sedimentary lithologies. Therefore, more samples of the Hart Jaune terrane would yield a more accurate representation of the crustal origins of this terrane, as compared to the Berthé terrane.

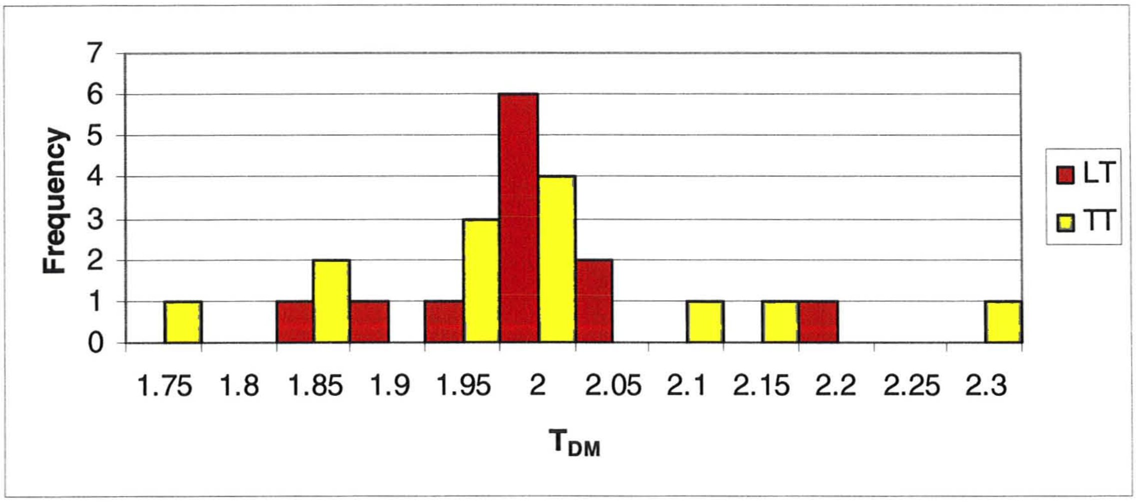

Figure 4.2: Lelukuau and Tshenukutish Terrane T_{DM} frequency comparison.

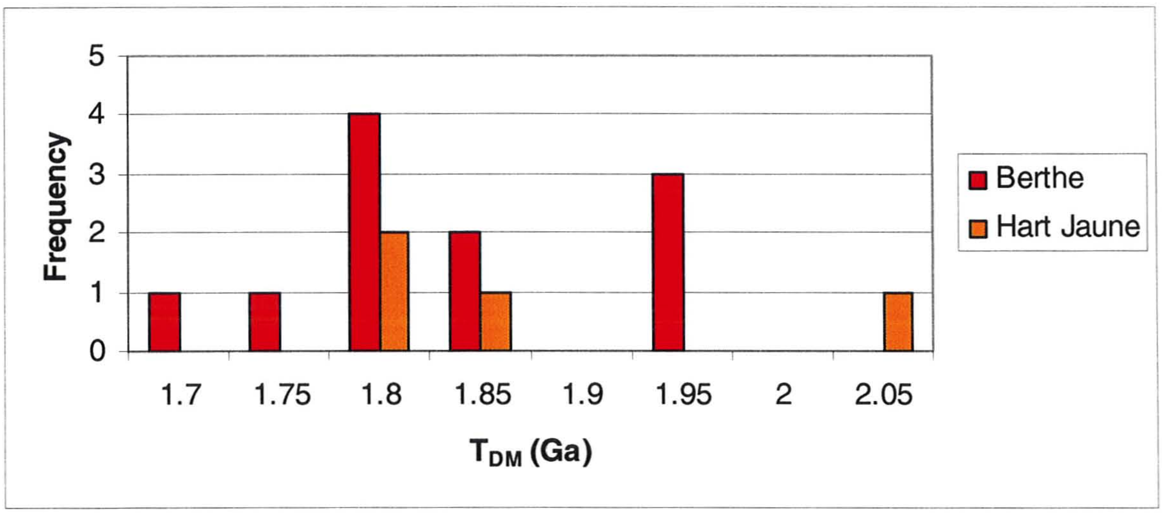

Figure 4.3: Hart Jaune and Berthé Terrane T_{DM} frequency comparison.

4.3 Terrane Boundary Modifications

In addition to the modification of the southwestern Gagnon Terrane boundary through the impact, which has been shifted to the west with the location of the ABT (mentioned in section 4.1), the Gagnon Terrane boundary has also been extended farther south. Like the location of the ABT, these modifications result from the Nd isotope model ages from samples southeast of the Manicouagan reservoir.

Further testing of the location of the ABT south of the impact is made possible by two samples, MQ1 and MQ2 (Figure 4.4), which are located in an area that has been previously interpreted as belonging to the Tshenukutish terrane of the MIZ. The model ages for these samples (1.71 and 1.84 Ga), although falling within the total range of the MIZ suite, are significantly younger than the majority of the model ages, and instead are more consistent with the Paleoproterozoic terrane (average 1.86 Ga), as opposed to the MIZ (average model age 2.12 Ga). The epsilon values of these samples add further evidence that they fit better with the Paleoproterozoic suite than the MIZ. The Epsilon value of MQ 1 is 3.3, which is the highest value of the Paleoproterozoic suite. As discussed in section 3.4, the Paleoproterozoic suite characteristically has higher epsilon values than the MIZ suite. Likewise, MQ 2 has an Nd concentration of 68.8 ppm which again is the highest Nd concentration of the Paleoproterozoic suite. Once more the MIZ suite characteristically has a lower Nd concentration than the Paleoproterozoic suite.

The geochemistry of these samples indicates that MQ 1 is well within the normal range of the Paleoproterozoic suite as it is located within the tonalite field. The MQ 2 chemistry is not as conclusive as MQ 1, being within the normal range of both the Paleoproterozoic and MIZ suites in the adamellite field. It is likely that the Berthé terrane continues farther northwest than originally expected (Figure 4.4). This means that the Tshenukutish terrane is pinched out between these two terranes, and is effectively confined to the interior of the impact crater. It is expected that the MIZ continues below the surface between the Archean basement wedge and the Paleoproterozoic thrust sheet overtop. However, there is no evidence south of the impact that this intermediate layer is present at the surface.

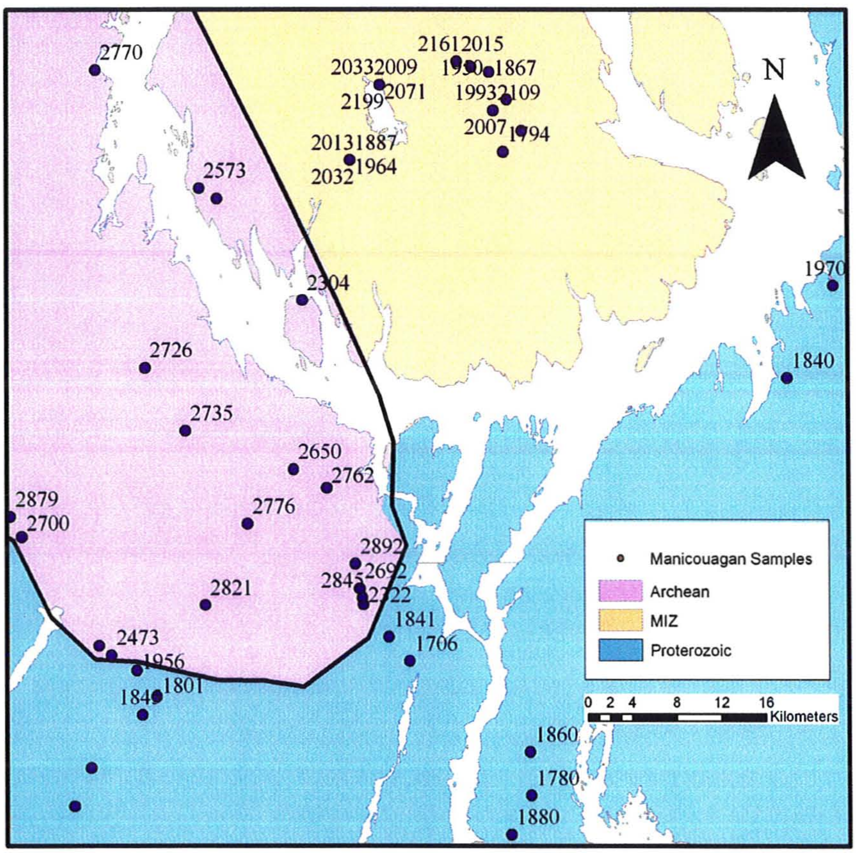

Figure 4.4: Nd model ages SW of the impact including MQ 1 and MQ 2 of the Paleoproterozoic crustal terrane

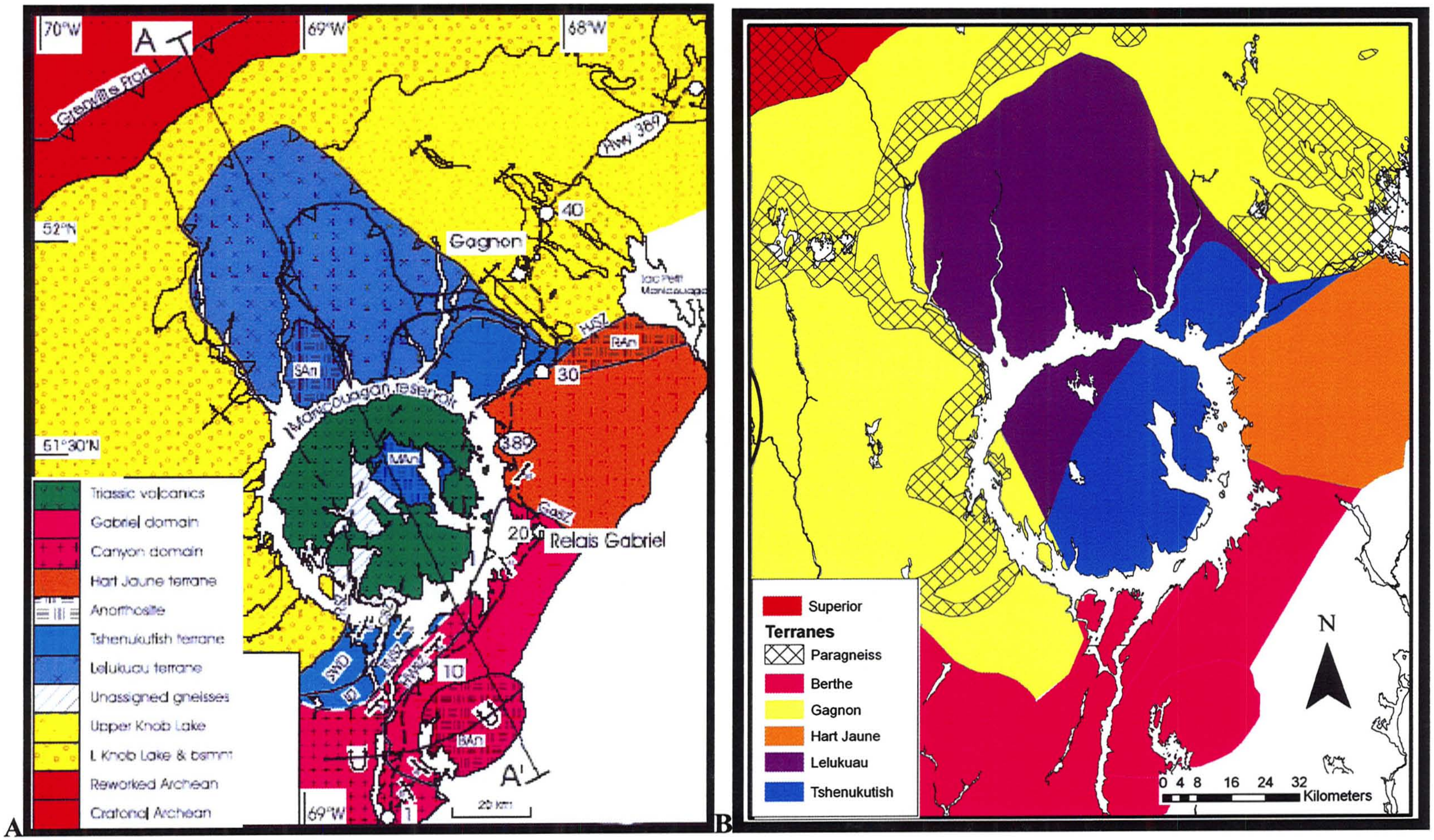

Figure 4.5: **A)** Previous terrane boundaries of the Manicouagan region (Hynes et al. 2000)
B) Modified terrane boundaries based on the Original crustal formation ages

CHAPTER 5: AEROMAGNETIC MAPPING

5.0 Introduction

Manicouagan, Quebec is fairly remote and therefore is not easily accessible for most of the year. Field work is limited to only summer months, at which time some of the area is still accessible only by helicopter. Due to these temporal and financial limitations, it is imperative to explore and compile as much information as possible about this site from remote resources, in order to gain an understanding of the area, as well as highlight specific areas of interest for focus during fieldwork.

5.1 Interpretation of Magnetic Data

Information obtained from the magnetic signatures in the region can be very helpful in understanding the lithology in the area (Figure 5.1) as the magnetic response often varies with lithological composition. This magnetic signal, demonstrated in the aeromagnetic mapping, is a result of many different factors.

As terranes experience geologic events, different magnetic patterns are imprinted onto the crust. The patterns of the magnetic signals in the Manicouagan region should vary between the Proterozoic allochthon and the Archean parautochthon, as they have different geologic histories.

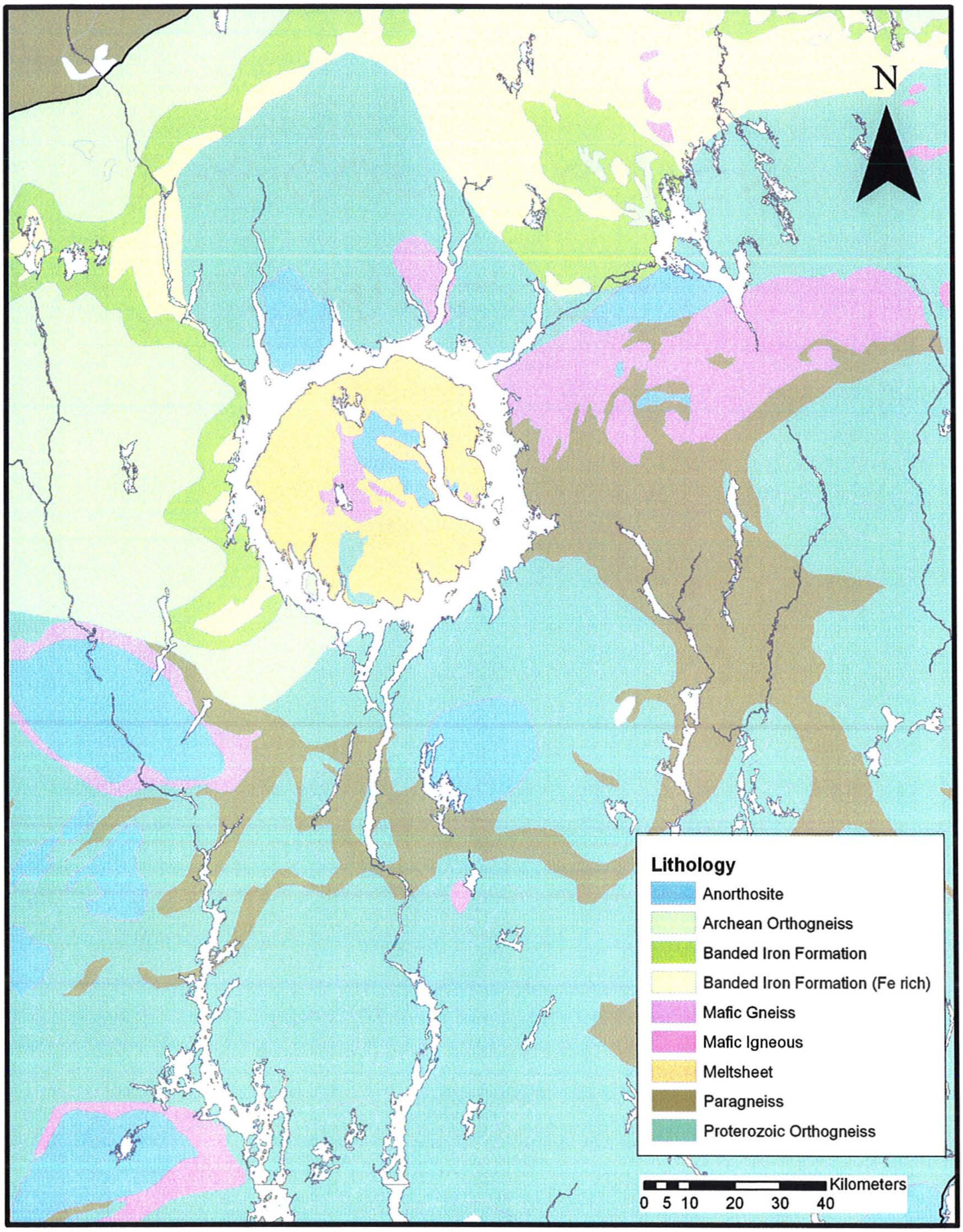

Figure 5.1: Lithologic Map of Manicouagan and surrounding area (after Davidson, 1998).

5.1.1 Archean Basement

The Archean terrane in the north was subject to the Kenoran metamorphism approximately 2.6 Ga following the cratonization of the Superior Province (Fleche et al. 2005). This resulted in a moderately deep level metamorphism that effectively homogenized the magnetic mineralogy and therefore the magnetic gradient. This may have occurred as the intense metamorphism elevated the minerals present above their Curie temperature, thus effectively resetting their magnetism and resulting in a crust with a low magnetic gradient (Clark, 1997). The resulting low gradient from the Archean parautochthon is illustrated in Figure 5.2.

In contrast to the Archean crust, the Proterozoic crust, which accreted to Laurentia after the Kenoran event, has a more complex magnetic signal, as it has not undergone this homogenizing event (Figure 5.2). In addition, it is composed of allochthonous terranes, with differing geologic histories. As a result of this variability of the magnetic gradients in the Manicouagan region, interpretation based on the lithologic differences of the crustal terranes in the area provides a more comprehensive understanding of the lithologic units present in the region. These units are: the Banded Iron Formation of the Gagnon Terrane, anorthosite massifs, mafic lithologies of the Hart Jaune Terrane, and the Manicouagan melt sheet.

5.1.2 Iron Formation on the Gagnon Terrane

The Gagnon terrane, located west of the impact, is characterized by a sedimentary sequence overlying Archean basement. Where the crust is pristine Archean crust, the magnetic signal reflects a typical low magnetic gradient. This becomes complicated on the eastern side of this terrane, where the signature of Archean crust has been overprinted with the presence of a Banded Iron Formation. The banded iron formation comprises a contrasting magnetic high of an iron rich suite (pink in Figure 5.2), surrounded by an iron poor region (blue and green in Figure 5.2). This formation stretches the length of the western side of the impact and, around the Proterozoic lobe to the north of the impact, and spreads out across the north eastern side of the study area (hatched pattern in Figure 5.2).

Towards the east of the Gagnon Terrane, the banded iron formation becomes indistinct, as this area is dominated by paragneiss. This sedimentary suite is responsible for a higher magnetic gradient. This is due to the mixture of magnetic minerals throughout the various sediments in the suite. The magnetic response is therefore highly dependent on the sedimentary facies variations as well its metamorphic grade (Clark, 1997).

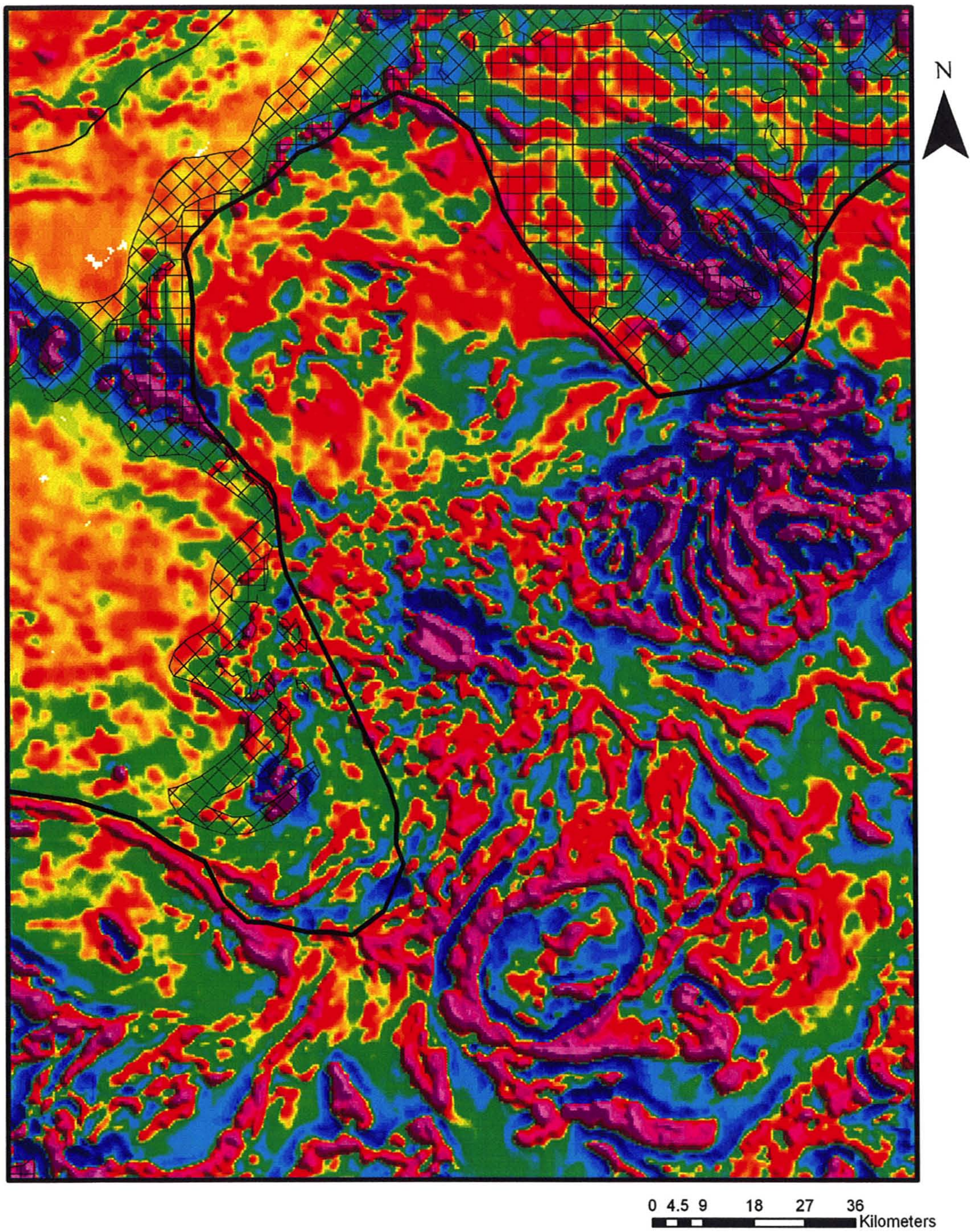

Figure 5.2: Quiet response of the Archean, overlain by the noisy response of the sediments on top. The thick black line represents the ABT. Pink and blue indicate the strongest magnetic gradient (>0.15 nT/km), and yellow and orange indicate the weakest magnetic gradient (<0.05 nT/km)

5.1.3 Anorthosite

There are large bodies of anorthosite in the region. These are mainly felsic in composition, and are distinct from the surrounding gneiss material as they are derived from a crustal re-melt. It is characterized by a lower magnetic gradient, surrounded by a stronger gradient. These are outlined in Figure 5.3

5.1.4 Mafic Lithologies of the Hart Jaune Terrane

Mafic suites are represented by high magnetic signals. This again is reasonable, as mafic rocks have high magnetite contents. These areas provide a large contrast with the anorthosite intrusions. The largest mafic suite is consistent with the Hart Jaune Terrane on the eastern side of the impact and is truncated to the north by the Hart Jaune fault.

It is also clear from Figure 5.4 that the Hart Jaune Terrane is distinctly allochthonous from the rest of the Proterozoic crustal body, as the folding patterns, or lineations are distinctly different from the rest of the linear patterns throughout this terrane indicated by a strong magnetic gradient surrounded by an intermediate gradient. This further supports the crustal history of this terrane, as it is the only terrane which remained at high crustal levels during the MIZ extrusion, and therefore was not involved in this metamorphic event.

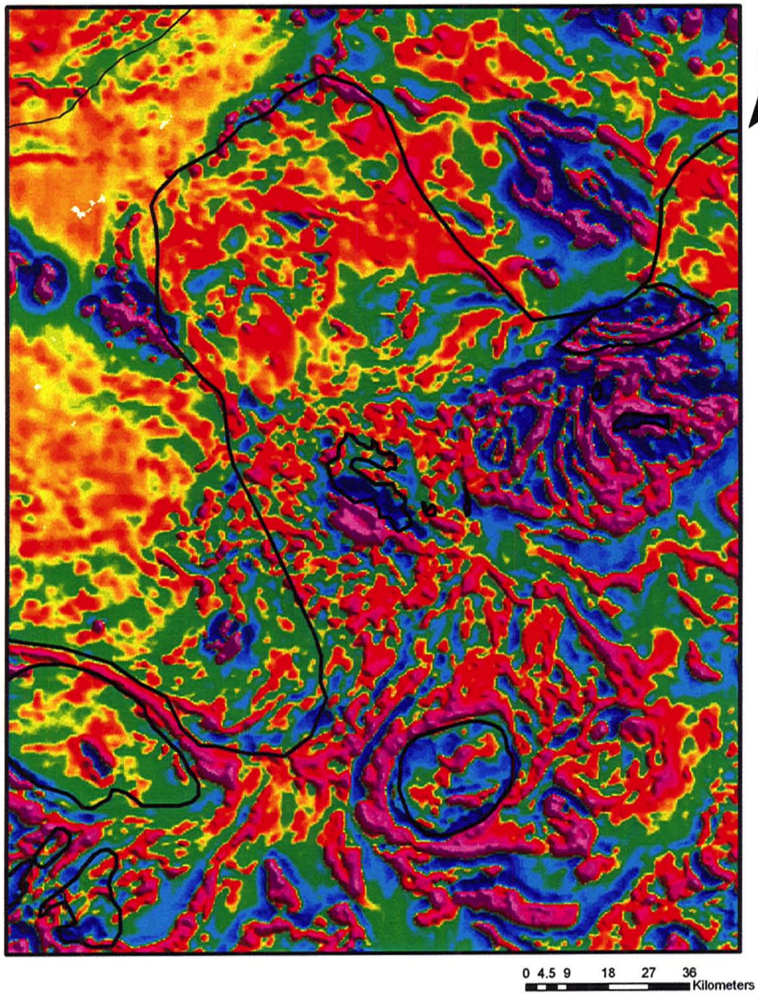

Figure: 5.3 Anorthosite intrusions amongst the Paleoproterozoic crust indicated by weaker magnetic gradient

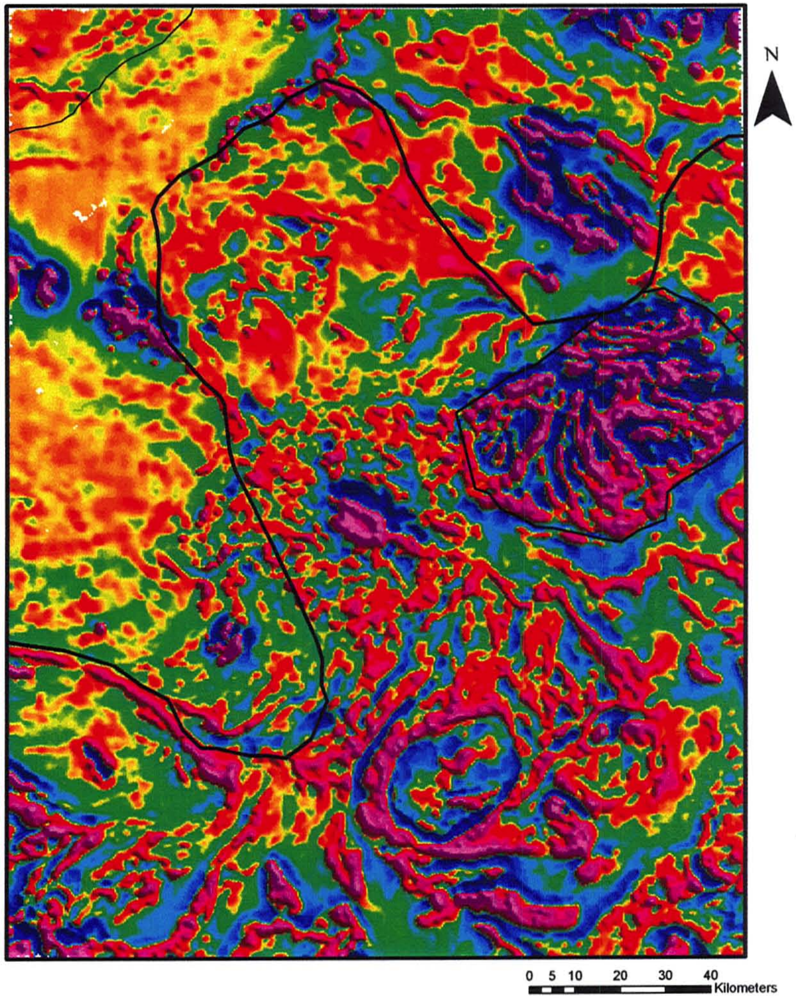

Figure 5.4 Distinct lineations of the Allochthonous Heart Jaune Terrane indicated by strong magnetic gradient.

5.1.5 Impact Structure

The magnetic signatures that represent the melt sheet in the interior of the impact crater displays a high magnetic gradient, outlining the central uplift, surrounded by a ring of lower gradient, which extends to the rim of the impact structure. McCall (2009) explains that this is a typical response for impact structures. The lower gradient of the ring is due to an increase in the porosity of the target rock, as fracturing within the target rocks is enhanced due to the hypervelocity event. The Manicouagan impact structure is modeled in this way in Figure 5.5.

CHAPTER 6: MANICOUAGAN HYPERVELOCITY IMPACT

6.0 Introduction

Understanding impacts and impact structures is imperative to understanding the early earth history of our planet. Since the Manicouagan impact has not undergone a large amount of post impact alteration, it may be particularly useful in helping to better understand other impacts that have undergone intense alteration, or impacts that are not accessible to direct study, such as those on other planetary bodies. Therefore, by studying the impacts on the earth surface, it is possible to gain a better understanding of a process which affects other planets in our solar system. In addition, as the Manicouagan impact is located in an area with a very complex geologic history, understanding this most recent event will help to reveal the evolutionary history that may be masked by the impact structure.

6.1 Impact Classification and Development

The velocity and size of the impact determines the complexity of the impact structure. Impact structures are classified into three categories, these are: simple craters, complex craters and multi-ringed basins. Simple craters include bowl shaped structures with a diameter of 2-4 km. Complex craters are larger than simple craters, and contain a central uplifted segment, surrounded by a trough. The largest impact structures are multi-ring basins, which contain several uplifted rings within the structure, surrounded by troughs, as the name suggests.

The process of crater formation has been summarized in many studies (Dressler and Reimold, 2001, Rondont, 1994, McCall, 2009) and is illustrated in Figure 6.1(A-F).

Contact and compression is the first phase of crater formation. When a projectile collides with the earth's surface (A), the energy is transmitted through the target rocks, pushing them downwards and outwards, thus creating a depression in the surface, termed a transient crater. Initially, little or no rock material escapes the impact site (Rondont, 1994).

The penetrating body is immediately deformed upon impact by compression, and will likely be vaporized completely. Rarely, the penetrating body is melted along with the surrounding target rocks and included in the melt rock that lines the depression (Rondont, 1994).

The force exerted upon the target rocks can lead to pressures greater than 100 GPa and temperatures reaching thousands of degrees within the first couple of seconds (Rondont, 1994). It is during this period that the largest shock pressures are reached for a hypervelocity impact event, leading to vaporization and melting (Spray and Thompson, 2008). Melting occurs as a result of excess energy, which is turned into heat, and melts the target rock. Below the impact site, pressures are lower i.e. 60 GPa, and crushing or brecciation of the target rock occurs, which facilitates the formation of dykes and veins through the target rock in the vicinity.

Following this is the excavation stage. Here, much of the melt and brecciated material within the crater is expelled from the impact and deposited elsewhere. This is accomplished through the dissipation of the initial kinetic energy from the contact and compression stage, which is partially converted to elastic waves traveling through the target rocks in a radial pattern (Dressler and Reimold, 2001)(C). Simultaneously, rarefaction waves are travelling in the opposite direction of the initial shock wave, releasing pressure, and aiding the expulsion of material.

Theoretically, a simple transient crater will reach a depth that is 1/3 of the structures diameter, with the rim of the structure elevated relative to the pre-impact topographic elevation. This ratio decreases with more complex structures, but the overall depth will increase, as more force is exuded upon the target rocks. The resulting structure is unstable however, and will immediately undergo modification to obtain a more stable structure (McCall, 2008).

Excavation is largely completed by the time of central uplift development in complex structures. The highly compressed material from the center of the impact floor begins to rebound, thus forming a bulge of material within the center of the structure. This describes the central uplift in larger complex structures, or rings in Multi-ringed basin structures (D).

The Crater Modification Stage is the final stage of the crater formation process (E). This is characterized by the gravitational collapse of the unstable central uplifted material, as well as collapse from the rim and walls of the crater itself, including both melted and unmelted material (McCall, 2009). This allochthonous material falls back into the trough of the impact structure, reducing the angles of the structure walls and therefore, creating a stable configuration. Faulting of the target rock around the rim of the original transient crater will facilitate this gravitational collapse as well (F). Thus, the depth of the structure is significantly reduced, while the diameter of the structure is appreciably increased (McCall, 2009).

The Manicouagan impact has been classified as a complex structure with a central uplift. This classification is based on field observations and measurements, as well as remotely sensed data. The melt material is believed to have a volume of 400-600 km^3, a depth of 230 m, and a diameter of 55 km across the Manicouagan Island. The average elevation of the melt sheet is 500m asl, with the central uplift reaching 590m asl (Spray and Thompson, 2008). The upper section of the melt is composed of medium grained material with no breccia inclusions. Below this, the melt becomes finer grained, with approximately 1% inclusions. The lowest layer of melt contains very fine to fine grained material with abundant clast material (Rondont, 1994).

Several cores have been obtained by drilling companies in order to gain a better understanding of the geology below the melt sheet rock. These have been located mainly in the center as well as the west side of the island. Through analysis of these cores, Spray and Thompson (2008) have concluded that the basal breccia of the impact rests on uneven basement rock. This is likely the result of faulting, which occurred below the melt sheet during the modification stage, but prior to the solidification of the impactite. Further analysis of these cores follows in this study, in order to better characterize the composition of the melt sheet material.

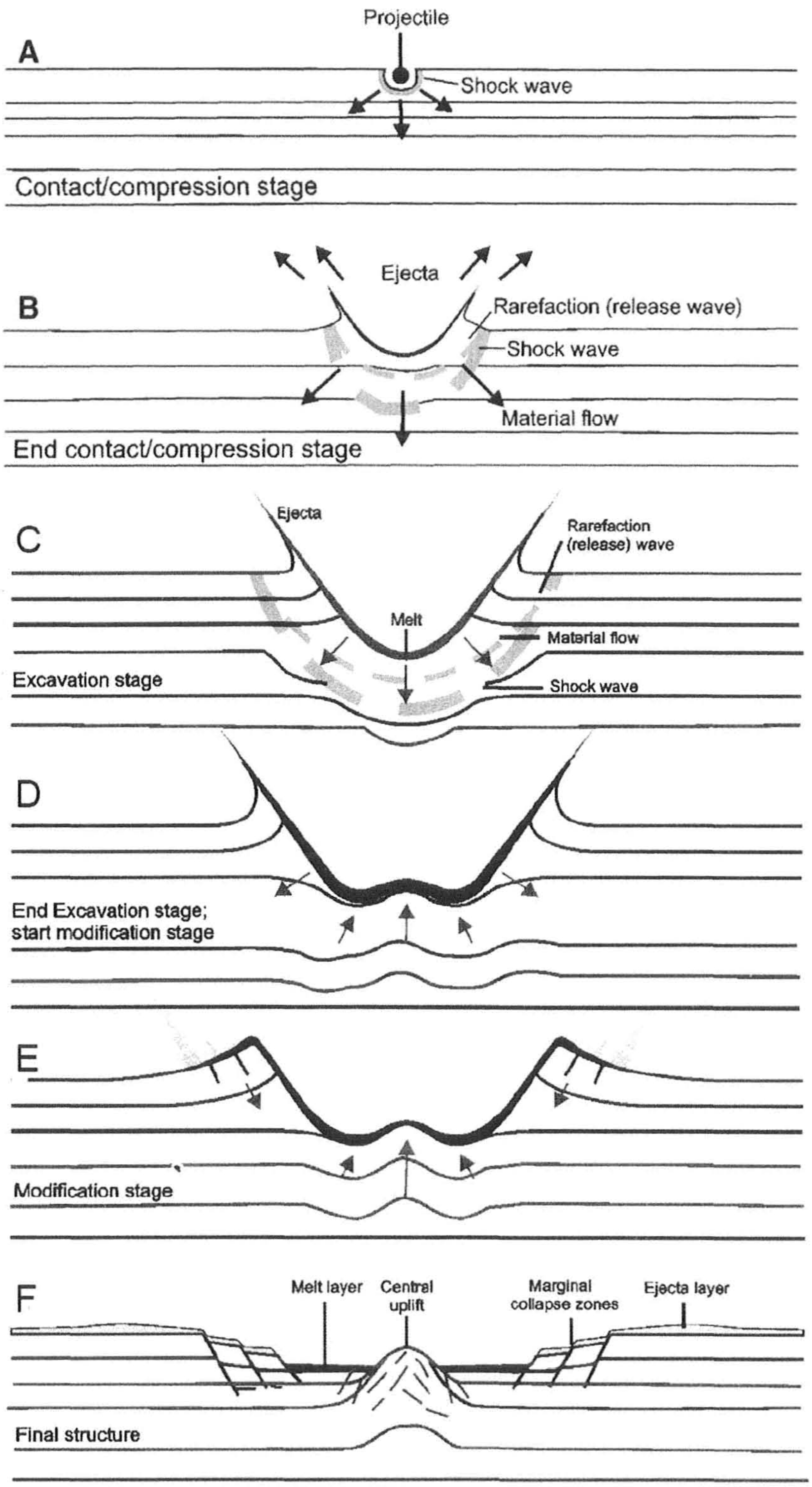

Figure 6.1: Step by step illustration of the formation of complex impact structures. (after McCall, 2009)

6.2 Isotopic Analysis of the Melt sheet

Core samples which include melt sheet samples were analyzed in terms of their Sr isotope ratios, in addition to the Nd isotope ratios, at McMaster University. These samples include the MIZ samples, a selection of Archean samples, three melt sheet samples and a few Paleoproterozoic samples, included as reference as these are not believed to underlie the melt sheet. Melt sheet samples which display differing amounts of differentiation were processed. This data is found in Tables 6.1-6.4.

6.2.1 Sr- Nd isotope comparison

The samples are again illustrated by their crustal suite, where Archean is represented in purple squares, MIZ is represented by orange triangles, and the Paleoproterozoic samples are represented by blue diamonds (Figure 6.2). The average ratios of each crustal body are indicated by the open symbols of the corresponding shape. The Nd isotope value is a weighted mean, taking into account the Nd concentration of each point. This was not possible for Sr, since no concentration data were available. The error bars on the Archean and MIZ means reflect two standard errors, and therefore include 95% confidence of the mean composition.

Since the composition of the melt sheet should reflect mixing of the target rock, its isotopic signature reflects a mixture of all crustal sources involved in the melt. It is not surprising then, that the melt sheet samples have the most intermediate distribution of the crustal suites, within the center of the plot. Interestingly though, the samples taken from the melt sheet are located between Archean mean and the MIZ mean. This distribution implies that there may be some Archean crust involved in the melt material.

A comparison of the Sr and Nd signatures in Figure 6.2 indicates that there is not only a distinct zonation of crustal suites on the Y-axis, but there is also a Sr isotopic difference between the Archean and MIZ crustal suites. The average Archean value, including two standard errors reflects a higher Sr ratio than the MIZ average values.

The Archean-MIZ mixing line suggests that this isotopic mixture is likely a result of 25% Archean, 75% MIZ material. However, closer examination of the data of the MIZ shows that it has a somewhat bimodal distribution, with a strong concentration of data points near the composition of the melt sheet. Therefore, the mean may not be representative of the actual target rocks in the impact. Hence the mixing model may not be reliable, indicating the necessity of further supportive evidence.

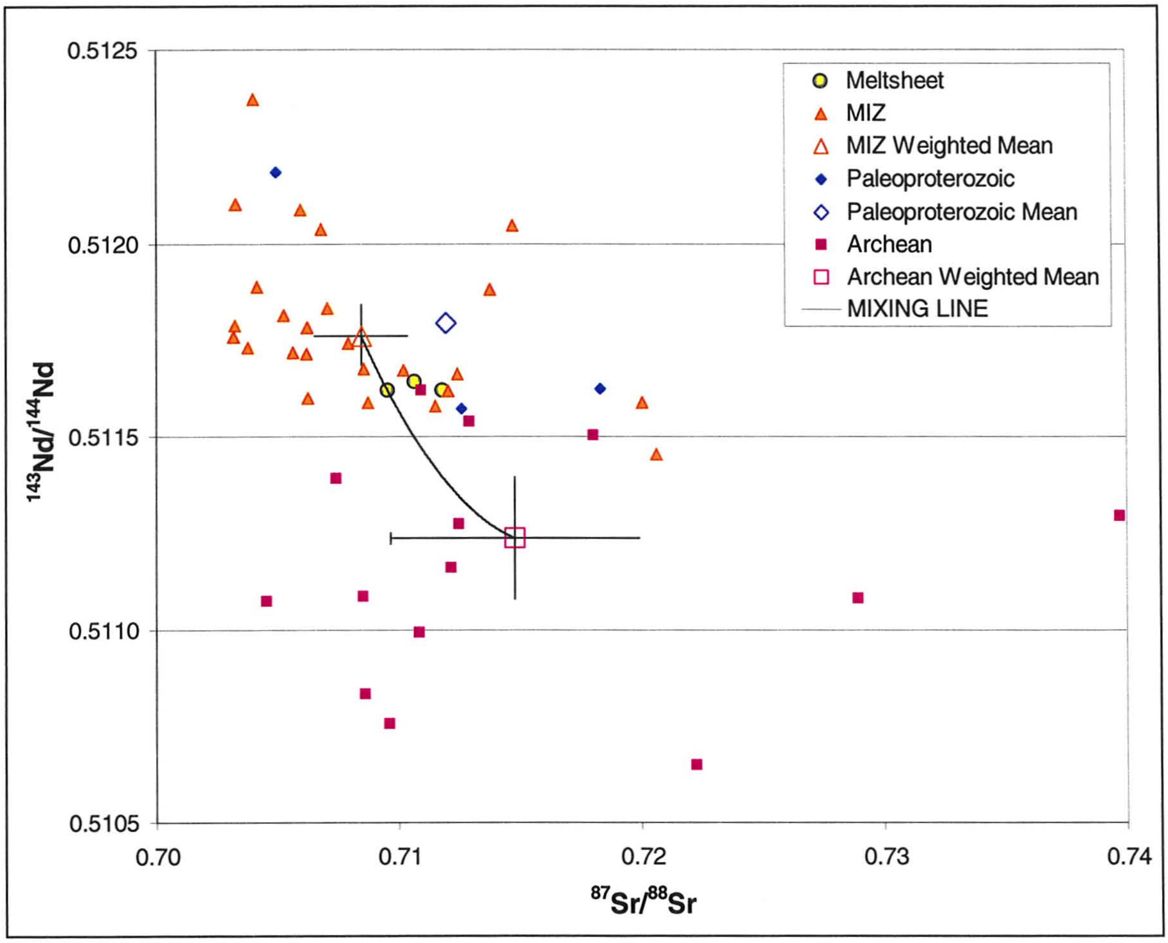

Figure 6.2: Comparison of Sr vs. Nd signatures from different crustal bodies in the Manicouagan study area.

6.2.2 Nd Concentration vs. Nd Ratio

A better understanding of mixing models may be obtained by plotting an isotope ratio against the elemental concentration of the tracer in question. Therefore the Nd isotope ratio is plotted against Nd concentration in Figure 6.3. Here, the Nd concentration of the Archean and the Proterozoic suites are very similar, and therefore Nd concentration is not especially diagnostic of crustal sources. Moreover, as differentiation has occurred within the melt sheet, the absolute values of the isotope concentration may not be a reliable indicator of melt sheet composition. For this reason, the Nd concentration of the melt sheet is not on the mixing line, as the Nd concentration of one sample will not represent the Nd concentration of the entire melt sheet. Nd isotopic ratios however, remained unchanged during differentiation, and therefore is still a reliable indicator.

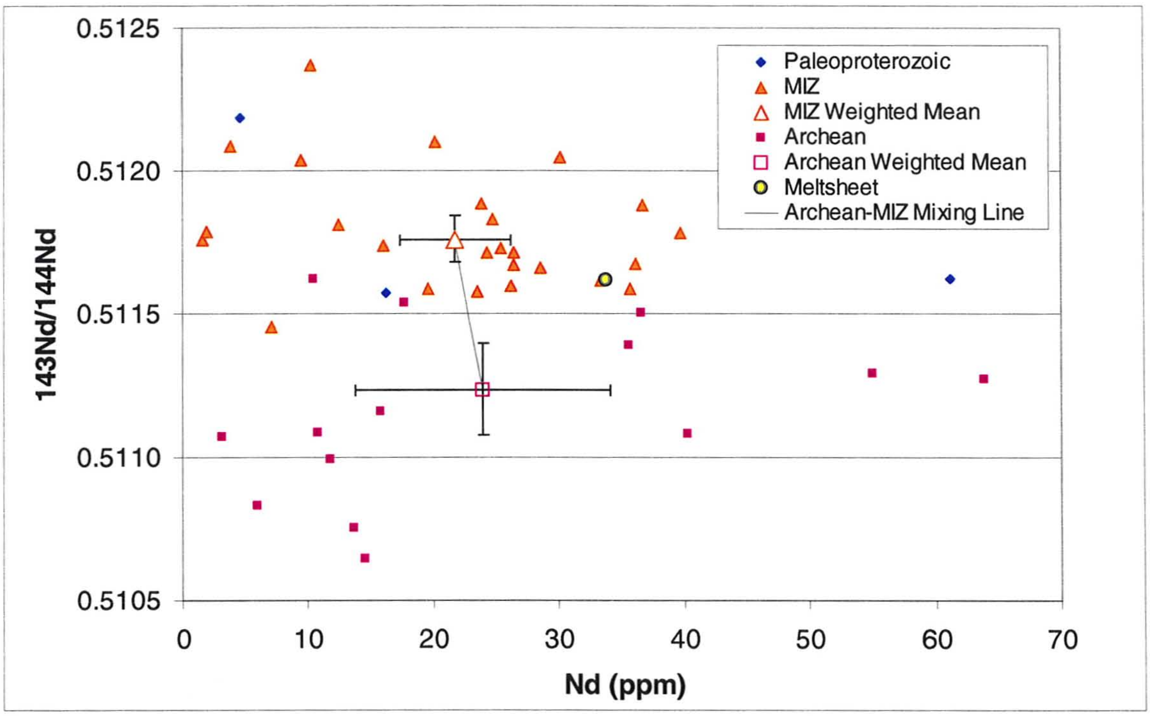

Figure 6.3: Nd isotopic ratio versus Nd elemental composition.

6.2.3 Isochron Diagram

In order to compensate for differentiation of the melt sheet, which affects elemental abundances, the Sm-Nd ratios of the crustal suites are evaluated with reference to the melt sheet composition. The Sm-Nd ratio should not be disturbed by magmatic differentiation since these are both highly incompatible elements, and therefore should produce a reliable representation of the mixing model.

Figure 6.4 shows the distribution of the MIZ and Archean suites on the Sm-Nd isochron diagram, with best fit-linear regressions and weighted mean computations also shown. This figure illustrates that the Sm-Nd signature for the melt sheet is located within the MIZ suite. The isotopic composition of the melt sheet is slightly less radiogenic than the MIZ mean, and therefore, it is possible that the target rocks may have included trace amounts of Archean crust. However, if this were the true, the sample should fall on the mixing line between the two weighted averages. As this does not occur, either the mean does not represent the target rocks, or differentiation occurred in the Sm-Nd system of the melt sheet. Since the most mafic melt sheet sample was analyzed, it follows, that this should be more radiogenic than other melt sheet samples. The average melt sheet composition would then fall to the left of the melt sheet sample in Figure 6.4, resulting in a composition with an even greater discrepancy from the MIZ mean isotopic composition. Because of this, it is likely the mean is not representative of the target rocks.

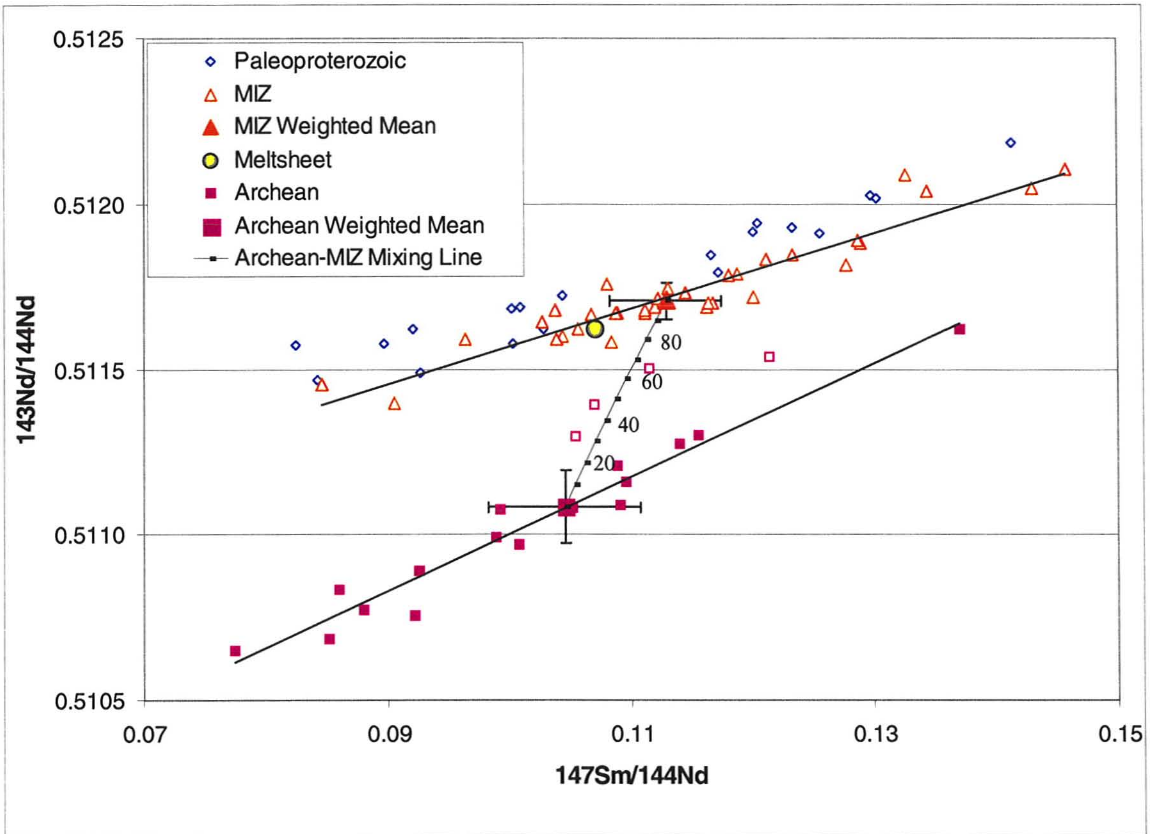

Figure 6.4: Archean isochron plotted with MIZ sample suite. Paleoproterozoic isochron included for reference. Melt sheet samples located within MIZ suite. Percentage of MIZ crustal component in the melt sheet is indicated with ticks on the mixing line.

6.2.3 Major Element Geochemistry

The geochemistry of the melt sheet indicates that there is a significant difference in the total value of silica in the MIZ compared to the Archean suite (Figure 6.5). Average values of each suite indicate that there is more silica in the MIZ than that in the Archean suite, therefore, analyzing the geochemical compositions of these as well as melt sheet samples may be useful in further determining the extent of Archean component within the melt sheet.

This suggests that there are other indicators in addition to isotopic analysis that can differentiate between crustal suites. However, since differentiation of the melt sheet is again an issue with major element concentrations, it is imperative to evaluate the geochemistry of the entire suite, as opposed to any single sample. A detailed analysis of this is outside the scope of this project.

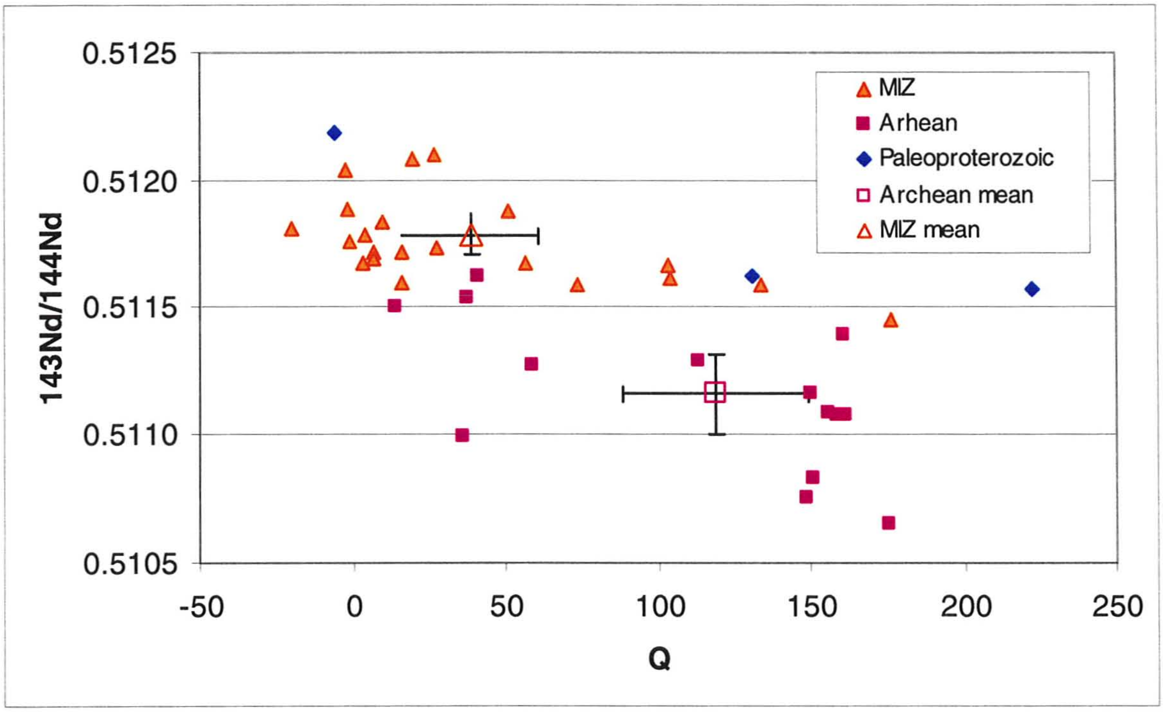

Figure 6.5: Petrochemical analysis of the MIZ and Archean samples, with Proterozoic measurements for reference.

Consequently, the results from this study are somewhat inconclusive in terms of the composition of target rock material. The data on the isochron diagram imply that the melt sheet can be produced solely by melting the MIZ, whereas the Nd-Sr isotope diagram imply that a small fraction of Archean crust may also be involved. In order to better characterize the composition of the melt sheet, Rb-Sr and Sm-Nd trace element data would need to be analyzed. In addition, major element analysis of the melt sheet may give an accurate depiction of the target rock material, as discussed above, and finally further isotopic analysis such as Pb-Pb studies may better describe the source of the melt sheet.

Table 6.1: Nd and Sr isotope data for the melt sheet samples

	Easting	Northing	Nd (ppm)	147Sm/144Nd	143Nd/144Nd	87Sr/86Sr	Q
Melt sheet							
0511-10	522 506	5 694 037			0.511642	0.71063	
0603-10	497 947	5 682 676	34		0.511620	0.70952	
0608-108	522 851	5 690 602			0.511620	0.71177	
MEAN					0.511627	0.71064	
ST. DEV					0.000013	0.00113	

Table 6.2: Nd and Sr isotope data for the Paleoproterozoic samples

	Easting	Northing	Nd (ppm)	147Sm/144Nd	143Nd/144Nd	87Sr/86Sr	Q
MQ1	515 211	5 641 038	16.2	0.0825	0.511573	0.71256	222
MQ2	513 320	5 643 250	61.2	0.1028	0.511623	0.7183	131
MQ27	492 459	5 637 894	4.5	0.1412	0.512184	0.70492	-6
MEAN					0.511793	0.71193	
ST. DEV					0.000339	0.00671	

Table 6.3: Nd and Sr isotope data for the Archean samples

	Easting	Northing	Nd (ppm)	147Sm/144Nd	143Nd/144Nd	87Sr/86Sr	Q
0513-11	496 359	5 683 606	17.7	0.1214	0.511538	0.71290	
MQ 3	511 057	5 646 151	35.6	0.1070	0.511391	0.70739	37
MQ 4	510 970	5 646 752	15.8	0.1096	0.511161	0.71214	160
MQ 5	510 710	5 647 591	14.5	0.0774	0.5106491	0.72225	150
MQ 6	510 327	5 649 818	13.7	0.0922	0.510757	0.70959	176
MQ 9	504 816	5 658 291	5.9	0.0860	0.510835	0.70859	149
MQ 11	495 082	5 661 754	11.8	0.0989	0.510993	0.71081	151
MQ 12	491 449	5 667 444	63.9	0.1140	0.511275	0.71245	36
MQ 16	496 834	5 646 102	10.4	0.1371	0.511621	0.71091	58
MQ 18	500 646	5 653 412	40.2	0.1052	0.511082	0.72891	41
MQ 33	480 321	5 652 265	3.1	0.1002	0.511075	0.70451	161
MQ 34	479 316	5 654 045	10.8	0.1091	0.511087	0.70849	159
MQ 30	488 389	5 641 594	55.0	0.1055	0.511295	0.73972	156
0509-A	505 634	5 673 483	36.6	0.1115	0.511503	0.71799	113
MEAN			23.9	0.1054	0.511162	0.71476	119
ST. DEV			19.0		0.000295	0.00961	54.7
2* ST. ERR			10.1		0.00015783	0.0051341	30.3

Table 6.4: Nd and Sr isotope data for the MIZ samples

	Easting	Northing	Nd (ppm)	147Sm/144Nd	143Nd/144Nd	87Sr/86Sr	Q
0301-A	519 588	5 694 978	7.1	0.0845	0.511454	0.72060	176
0301-B	519 589	5 694 979	26.4	0.1201	0.511718	0.70559	6
0301-C	519 590	5 694 980	25.4	0.1145	0.511731	0.70375	27
0302-A	524 083	5 691 570	36.1	0.1112	0.511676	0.70854	3
0501-A	523 722	5 686 894	3.8	0.1326	0.512087	0.70592	19
0506-A	509 940	5 686 130	36.6	0.1289	0.511881	0.71374	51
0506-B	510 940	6 686 130	33.3	0.1056	0.511619	0.71202	104
0506-C	511 940	7 686 130	28.5	0.1067	0.511663	0.71240	103
0506-D	512 940	8 686 130	26.2	0.1044	0.511599	0.70621	16
0506-E	513 940	9 686 130	19.6	0.0963	0.511589	0.70869	73
0511-A	522 506	5 694 037	9.4	0.1344	0.512038	0.70678	-2
0511-B	523 506	6 694 037	0.4	1.0274	0.511688	0.70304	7
0511-C	524 506	7 694 037	1.6	0.1081	0.511758	0.70317	-1
0602-A	512 647	5 692 881	12.4	0.1277	0.511814	0.70522	-21
0602-B	512 648	5 692 882	23.8	0.1286	0.511888	0.70413	-2
0602-C	512 649	5 692 883	35.7	0.1038	0.511588	0.72000	134
0602-D	512 650	5 692 884	24.8	0.1211	0.511833	0.70703	10
0608-A	522 850	5 690 601	26.4	0.1088	0.511671	0.71018	57
0608-B	522 851	5 690 602	39.7	0.1180	0.511783	0.70617	4
0608-C	522 852	5 690 603	24.2	0.1121	0.511715	0.70616	16
0608-D	522 853	5 690 604	20.1	0.1457	0.512103	0.70326	27
0303-12	525 402	5 688 742	10.2	0.1806	0.512373	0.70399	
0502-09	520 880	5 694 490	23.5	0.1083	0.511580	0.71149	
0511-30	522 506	5 694 037	1.9	0.1187	0.511789	0.70321	
0511-31	522 506	5 694 037	16.0	0.1131	0.511742	0.70787	
0302-11	524 083	5 691 570	30.1	0.1429	0.512048	0.71467	
MEAN (M)			20.9	0.1191	0.511786	0.70822	38
ST. DEV			11.8		0.000205	0.00492	51.7
2*ST. ERR			4.6		8.03538E-05	0.0019292	22.6

CONCLUSIONS

The evolutionary history of Manicouagan Quebec is complex and multidimensional. Through analysis of the isotopic composition of distinct crustal terranes, the boundaries of these terranes have been delineated in areas where the boundaries were previously unclear.

Nd model age mapping south of the impact structure has indicated that the extent of the Gagnon terrane continues farther south than previous identified in previous models. In addition, this model reveals that the Paleoproterozoic crust of the Berthé Terrane continues farther eastward than indicated in past studies as well, effectively truncating the Tshenukutish Terrane of the MIZ south of the reservoir. The result of this is the reconfiguration of the boundaries south of the impact structure.

The calculation of Nd model ages becomes complex within the MIZ, as this area does not reflect a true crustal forming event. Instead the crustal composition reflects Paleoproterozoic magma which was contaminated with Archean crust, resulting in crustal characteristics of both Proterozoic and Archean material throughout the terranes of the MIZ. This mixing is also apparent in the bordering Archean crust to the west, giving further evidence of a mixed crustal source.

Since the portion of the ABT running through the impact structure is defined by the boundary between the MIZ and Archean crust, some degree of crustal mixing was found throughout both sides of this boundary. Therefore the location of the ABT was delineated in this area using Nd isotope analysis to differentiate the amount of Archean influence in the crust. This more precise location is west of that proposed in earlier studies.

Differentiation between the Lelukuau Terrane and the Tshenukutish Terranes of the MIZ is not possible through Nd isotope analysis as these terranes likely come from the same crustal material. The melt sheet was primarily generated by melting of the MIZ, however it may contain a small amount of Archean crust (<25%). The amount of Archean influence in its crustal makeup has not been fully quantified, as the results from this study are somewhat conflicting. This study was successful in identifying distinctive characteristics of the possible crustal sources. Such characteristics include: the distribution of trace element signatures within each crustal terrane and the composition of major elements, and therefore the silica composition in each crustal terrane. This information can be utilized in future analyses, and therefore the composition of the melt sheet can be further quantified.

The isotopic ratio of the melt sheet reveals information on the influence of hypervelocity impacts on the surrounding geology and therefore evolutionary history of the area. The isotopic signatures in the melt sheet suggest that the depth of the melting has been limited to the shallow wedge of the MIZ material. This is further supported with the delineation of the ABT through the impact structure, as the processes included in the collision and formation of a complex structure did not alter the path of the ABT. Therefore, the amount of influence a hypervelocity impact event is limited to the localized modification of the target rock, but does not modify boundaries or support horizontal transport of the target rock material.

REFERENCES

Arndt, N.T. and Goldstein, S.L. 1987. Use and abuse of crustal formation ages. Geolgy. 15:893-895

Carr, S.D. Easton, R.M. Jamieson, R.A, Culshaw, N.G. 2000. Geologic transect across the Grenville orogen of Ontario and New York. Canadian Journal of Earth Science. 37:193-216

Clark, D.A. 1997. Magnetic petrophysics and magnetic petrology; aids to geological interpretation of magnetic surveys. Journal of Austrailian Geology and Geophysics. 17(2): 83-103

Cox, R.A. Indares, A. Dunning, G.R. 2002. Temperature-time paths in the high-P Manicouagan Imbricate zone, eastern Grenville Province: Evidence for teo metamorphic events. Precambrian Research. 117: 225-250

Davidson, A (comp.) 1998: Geological map of the Grenville Province, Canada and adjacent parts of the Unites States of America; Geological Survey of Canada, Map 1947 A, scale 1:2,000,000.

Davison, A. 1998. An overview of Grenville Province geology, Canadian Shield; Chapter 3 in Geology of the Precambrian Superior and Grenville Provinces and Precambrian Fossils in North America, (co-ord.) S.B. Lucas and M.R. St-Onge; Geological Survey of Canada, Geology of Canada, 7: 205-270

Debon, F. and Le Fort, P. 1982. A chemical-mineralogical classification of common plutonic rocks and associations. Transactions of the Royal Society of Edinburgh: Earth Science. 73: 135-149

DePaolo, D.J. 1981. Neodymium isotopes in the Colorado Front Range and crust mantle evolution in the Proterozoic. Nature. 291: 193-197

DePaolo, D.J. and Wasserberg, G.J. 1976a. Nd variations and petrogenic models. Geophysics Research Letters. 3:249-252

Dickin, A.P. 2005 Radiogenic Isotope Geology. 2nd ed. Cambridge: Cambridge Uniersity Press: pp 15-35, 70-100, 174-202

Dickin, A.P. 2000. Crustal formation in the Grenville Province; Nd-isotope evidence. Canadian Journal of Earth Science. 37:165-181

Dickin, A.P. and McNutt, R.H. 2007. The Central Medisedimentary Belt (Grenville Province) as a failed back-arc rift zone: Nd isotope evidence. Earth and Planetary Science Letters. 259:97-106

Dressler, B.O. Reimold, W.U. 2001. Terrestrial impact melt rocks and glasses. Earth-Science reviews. 56:205-284

Easton, D.W. Hynes, A. Indares, A. Rivers, T. 1995. Seismic images of eclogites, crustal-scale extension, and Moho relief in the eastern Grenville province, Quebec. Geology. 23(9): 855-858

La Fleche, M.R. Birkett, T.C, Corriveau, L. 2005. Crustal development at the pre-Grenvillian Laurentian margin: a record from contrasting geochemistry of mafic and ultramafic orthogneisses in the Chochocouane River area, Quebec. Canadian Journal of Earth Science. 42: 1653-1675

Hanmer, S. Corrigan, D. Pehrsson, S. Nadaeu, L. 2000. SW Grenville Province, Canada; the case against post-1.4 Ga accretionary tectonics. Tectoniphysics. 319: 33-51

Hynes, A. Eaton, D. 1999. Lateral ramps as an aid to the unroofing of deep-crustal rocks: Seismic evidence from the Grenville province. Tectonics. 18(2): 343-360

Hynes, A. Indares, A. Rivers, T. Gobeil, A. 2000. Lithoprobe line 55: integration of out-of-plane seismic results with surface structure, metamorphism, and geochronology, and the tectonic evolution of the eastern Grenville Province. Canadian Journal of Earth Science. 37: 341-358

Hynes, A. St. Jean, A. 1997. Metamorphic signatures of faulting in the Manicouagan Reservoir region, Grenville Province, Eastern Quebec. The Canadian Mineralogist. 35:1173-1189

Indares, A. Dunning, G. Cox, R. 2000. Tectono-thermal evolution of deep crust in a Mesoproterozoic continental collision setting: the Manicouagan Example. Canadian Journal of Earth Science. 37: 325-340

Indares, A. 2003. Metamorphic textures and P-T evolution of high-P granulites from the Lelukuau terrane, NE Grenville Province. Journal of Metamorphic Geology. 21:35-48

Indares, A. White, R.W. Powell, R. 2008. Phase equilibria modeling of kyanite-bearing anatectic paragneiss from the central Grenville Province. Journal of Metamorphic Geology. 26: 815-836

Indares, I. Dunning, G. 2004. Crustal architecture above the high-pressure belt of the Grenville Province in the Manicouagan area: new structural, petrologic and the U-Pb age constraints. Precambrian Research. 130: 199-228

Indares, A. Dunning, G. Cox, R. Gale. 1998. High-pressure, hig –temperature rocks from the base of thick continental crust: Geology and age constraints from the Manicouagan Imbricate Zone, eastern Grenville Province. Tectonics. 17(3):426-440

Jordan, S.L. Indares, A. Dunning, G. 2006. Partial melting of metapelites in the Gagnon terrane below the high-pressure belt in the Manicouagan area (Grenville Province): pressure-temperature (P-T) and U-Pb age constraints and implications. Canadian Journal of Earth Science. 38: 1309-1329

Martin, C. and Dickin, A.P. 2005. Styles of Proterozoic Crustal Growth on the southeast margin of Laurentia: Evidence from the central Grenville Province northwest of Lac-St. Jean, Quebec. Canadian Journal of Earth Science. 42(10): 1643-1652

McCall, G.J.M. 2009. Half a century of progress in research on terrestrial impact structures: A review. Earth Science Reviews. 92: 99-116

McCulloch and Wasserburg, 1978. Sm-Nd and Rb-Sr chronology of continental crust formation. Science 200: 1003-11

Milligan, P.R, Gunn, P.J. 1997. Enhancement and resentation of airborne geophysical data. Journal of Austrailian Geology and Geophysics. 17(2): 83-103

National Topographic Data Base (NTDB) 2006. Scale 1:250,000, Received from Lloyd Reeds Map Collection ~ MCMaster University Library (Grid Zones obtained 12H-P, 13A-L, 21M, 22C-P. 31B-P, 41H 1, 32(6), 23(5))

Natural Resources Canada (NRC), 2008-07-28, Geosciences Data Repository. http://edg.rncan.gc.ca/aeromag/index_e.php.2008-05-15

Rivers, T. and Chown, E.H. 1986. The Grenville Orogen in Eastern Quebec and Western Labrador – Definision, Identification and Tectonometamorphic Relationships of Autochthonous, Paratochthonous, and allochthonous Terranes. The Grenville Province, edited by J.M.Moore, A. Davidson, A.J Baer. Geological Association of Canada Special Paper 31: 31-50

Rivers, T. Martignole, J. Gower, C.F. Davidson, A. 1989. New Tectonic Divisions of the Grenville Province, Southeast Canadian Shield. Tectonics. 8: 63-84

Rivers, T. 1997. Lithotectonic elements of the Grenville Province: review and tectonic implications. Precambrian Research. 86: 117-154

Spray, J.G. and Thompson, L.M. 2008. Constraints on central uplift structure from the Manicouagan impact crater. Meteoritics and Planetary Science. 43(12): 2049-2057

Wynne-Edwards, 1972. The Grenville Province. Variations in Tectonic Styles in Canada. Geological Association of Canada Special Paper. 11: 263-334

APPENDIX A: ANALYTICAL METHODS

A1. Field Sampling

Obtaining the rock samples for isotopic analysis was completed in two stages. The first was on site in Manicouagan, where homogeneous grey gneiss which represents the country rock in the area was harvested. The rock samples were collected from exposed outcrop along the highways and logging roads. As previously mentioned, samples that have undergone weathering or alteration will not produce accurate results, and therefore were excluded from our collection.

The second set of sampling took place at the department of Forestry and Geology at the University of New Brunswick (UNB). Here core samples from within the impact crater were obtained for analysis.

A.2 Rock Crushing

A.2.1 Samples from Outcrops

Once the rock arrived at McMaster University, it was crushed into a usable powder. First, the rock was scrubbed with a course wire brush in order to remove sediment that may have adhered to any fresh surface. Following this, any remaining segments of the rock that were unusable, such as weathered surfaces or that contain intrusions which do not characterize the original country rock, were removed in order to obtain the most reliable results. The rock was then cut into one inch cubes using a hydraulic splitter, and fed into a mechanical jaw crusher, which crushed the cubes into gravel sized particles. This sample was sorted through a table top sample splitter to ensure a randomly sorted sample, approximately one third of the total sample size. This portion was loaded into a disc mill and shatter box, which ground the sample into a fine powder ready for dissolution.

Each machine involved in the process was thoroughly cleaned between each sample, in order to prevent contamination.

A.2.2 Core samples

The core samples that were obtained from UNB were first washed in a sonic bath. The purpose of this was to dislodge any metal that may have adhered to the core sample during the cutting process. This was also effective in removing any sediment or dirt that was on the core samples as well. Following this, the samples were split, crushed and powered in the process outlined above.

A.3 Chemical Dissolution

Approximately 0.2g of the sample was weighed into a teflon bomb. In order to analyze the isotopic signature, the trace elements must be separated from within the rock. In order to dissolve these rock forming materials which make up the silica rich rock matrix, the sample was dissolved in 10mL of concentrated hydrofluoric acid, baked in the oven at 140C° for four days. The sample was evaporated on hot plates until completely dry. Unfortunately, this process often causes the formation of insoluble sulfates, and therefore, the sample was dissolved in 5mL of concentrated nitric acid in order to avoid this. Again this solution was evaporated on hotplates. Finally 5 mL of Hydrochloric acid was poured into the bomb and it is again baked at 140C° for 24 hours.

The resulting solution was diluted with 10 mL of filtered milliQ, and 5 mL of the 15mL solution was decanted into a second sample container and marked as an ID (for isotope dilution), while the remaining 10mL solution became the sample IR (isotope ratio). The ID was spiked with 0.2mL of and enriched ^{150}Sm and ^{149}Nd isotope solution, while the IR remained unspiked, representative of the true isotopic ratio of the rock sample for isotope analysis. Both aliquots were set under hot lamps to evaporate.

A.4 Column Chemistry

The samples were re-dissolved into 2 mL of 1M HCl, centrifuged in order to separate any remaining undissolved sediment, and 1 ml of the solution was loaded into a cation exchange column. Once loaded, the sample was eluted with a series of 1 mL, 3 mL, and 48 mL of 3M HNO_3, before the Rare Earth Elements (REE) were collected through a final step of 12ml of 7.5M HNO_3. This sample was again dried under the hot lamps, and dissolved in 0.3M HCl. The solution was loaded into the REE columns, where the REEs were further separated in order to collect, more precisely, the Nd and Sm elements. This step is also particularity important as it decreases opportunities for isobaric interferences in mass spectrometry such as ^{144}Sm with ^{144}Nd. The chemical separation was accomplished through 'reverse phase' method, where a series of dilute mineral acids are eluted through the columns: 0.3M HCl was washed through the columns in stages involving 1 mL, 3 mL, and 25 mL, then finally the Nd was collected through a final step where 12 mL of 0.3M HCl eluent. Following this, the IDs had an additional 2.5 mL of 1M HCl, before the Sm REE was collected through 12 mL of 1M

HCl. The IR and the IDs were evaporated until they were almost dry before they were loaded into the Mass Spectrometer.

A.5 Mass Spectrometry

Double filament beads are used in mass spectrometry where volatilization and ionization of a sample do not occur at the same temperature. In Nd isotope analysis, samples are loaded onto the side filament, made of tantalum, with a 0.3M H_3PO_4 loading solution. Here the samples undergo volatilization, while the center rhenium filament promotes ionization at a higher temperature. In the case of Sr isotope analysis, a single tantalum filament is used as volatilization and ionization occur simultaneously. This method of ionization through intense heat under vacuum is called Thermal Ionization Mass Spectrometry (TIMS). All samples were processed in this manor on a VG isomass 354 mass spectrometer.

IRs that had a running precision greater than 0.01‰, and IDs with a running precision greater than 0.02% were rejected, therefore ensuring the analytical uncertainty of the model ages to be within 20 Ma (Dickin and McNutt, 1989).

APPENDIX B:
Table B.1: La Jolla Standards

Date	**$^{143}Nd/^{144}Nd$**	**Standard Error (‰)**
10/15/2007	0.511874	0.012
1/21/2008	0.511845	0.012
2/18/2008	0.511839	0.012
3/17/2008	0.511822	0.013
4/7/2008	0.51185	0.013
8/18/2008	0.511833	0.01
8/21/2008	0.511879	0.011
11/20/2008	0.511859	0.01
11/24/2008	0.511853	0.013
11/24/2008	0.511866	0.011
1/12/2009	0.511877	0.011
3/16/2009	0.511867	0.012
3/23/2009	0.511867	0.016
4/20/2009	0.511868	0.013
4/23/2009	0.511884	0.017
6/22/2009	0.511852	0.011
MEAN and POP. SD	0.511858	0.000018

APPENDIX C: AEROMAGNETIC MAPPING PROCEDURE

The Aeromagnetic data was obtained from the Geological Survey of Canada (GSC) through Natural Resources Canada (NRC, 2008), and was processed using the program Geosoft OASIS. This data was downloaded in a specified WGS 84 projection and therefore was ready for processing immediately.

The data was first micro-leveled so as to remove any error that may have occurred during recording due to movement of the plane. This process resulted in an error or noise grid which was subtracted from the original, leaving a corrected version of the magnetic dataset.

Following the microleveling, the magnetic data was reduced to its magnetic poles. This process shifts the signal from an oblique angle to vertical, shifting anomalies that are asymmetrically related to their sources to the magnetic inclination and declination of the study area (Milligan and Gunn, 1997). This effectively centers the signal response so that it is perfectly vertical over the magnetic anomaly.

This map was filtered once again with an upward continuing filter of 800 m, in order to highlight the high frequency response from the near surface. The first vertical derivative of this resulting image was then calculated, which removes regional trends from the dataset. This first derivative of the upward continued aeromagnetic data provided the basis for interpretation for this study.